

# 1 **Reconstructing fluvial incision rates based upon palaeo-water tables** 2 **in Chalk karst networks along the Seine valley (Normandy,** 3 **Northern France)**

4 Carole Nehme<sup>1</sup>, Andrew Farrant<sup>2</sup>, Daniel Ballesteros<sup>1</sup>, Dominique Todisco<sup>1</sup>, Joel Rodet<sup>3,4</sup>, Diana Sahy<sup>2</sup>, J.  
5 Michael Grappone<sup>5</sup>, Jean-Claude Staigre<sup>4</sup>, Damase Mouralis<sup>1</sup>.

6 1 University of Rouen Normandy, IDEES UMR 6266 CNRS, Mont Saint-Aignan, France

7 2 British Geological Survey, Keyworth, Nottingham, NG12 5GG, United-Kingdom.

8 3 University of Rouen, M2C Laboratory UMR 6143 CNRS, Mont Saint-Aignan, France

9 4 Centre Normand d'Étude du Karst, CNEK, Rouen, France.

10 5 Geomagnetism Laboratory, University of Liverpool, Liverpool L69 7ZE, United-Kingdom.

11 **Keywords:** Karst, cave levels, Chalk, paleomagnetism, U/Th dating, Seine River, landscape evolution.

12 Corresponding author: [carole.nehme@univ-rouen.fr](mailto:carole.nehme@univ-rouen.fr)

## 14 **Introduction**

15 Determining rates of landscape evolution, river incision and continental uplift are important prerequisites  
16 for modelling landscape change over 10<sup>2</sup>-10<sup>6</sup> year timescales. However, quantitative estimates of landscape  
17 change are often hampered by the lack of datable material or preserved ancient deposits, especially in areas  
18 of rapid erosion or weathering. Cave systems are useful tools for reconstructing the landscape evolution  
19 because they can record the elevation of palaeo-water tables, which are controlled by fluvial base levels in  
20 many karst areas (Palmer, 1987). Moreover, cave deposits can be accurately dated using a variety of  
21 techniques, notably uranium series (Bischoff *et al.*, 1988), palaeomagnetic dating (Sasowsky *et al.*, 1995)  
22 and burial (<sup>26</sup>Al/<sup>10</sup>Be) dating (Granger *et al.*, 2001). Cave systems also have the benefit that they, and the  
23 deposits they contain, can be preserved over long timescales where surface landforms such as river terraces  
24 may be degraded by weathering and erosion. Therefore, mapping and dating cave systems can be used to  
25 deduce valleys incision rates and continental uplift (Farrant *et al.*, 1995; Granger *et al.*, 2001; Rossi *et al.*,  
26 2016). In this paper, the landscape evolution of the western Paris Basin (France) was investigated through  
27 the systematic investigation of relict caves exposed in the sides of the lower Seine River valley around  
28 Rouen (Eastern Normandy).

29 Cave passage morphology can be used to determine palaeo-water table by identifying the transition from a  
30 vadose to a phreatic morphology (Palmer, 1987, 1991; Atkinson and Rowe, 1992). Caves formed above the  
31 water table are typified by steeply descending narrow canyons and shafts, whilst those formed beneath the  
32 water table are characterized by rounded conduits, often with a looping profile (Lauritzen 1985; Ford and  
33 Williams, 2007). In a phreatic environment, the palaeo-water table can also be identified from the elevation  
34 of concordant phreatic loop crests and phreatic avens and lifts, or where horizontal water table passages cut  
35 across dipping strata. However, true water table caves are relatively uncommon (Gabrovšek *et al.*, 2014).

36 In carbonate terrains, as rivers incise their valleys, the corresponding drop in base level causes the water  
37 table to fall and leads to the subsequent abandonment of shallow-phreatic conduit networks, creating new  
38 conduit networks at lower elevations (Ford and Williams, 2007; Audra and Palmer, 2013). During phases

39 of static base level, or when cave formation is restricted to certain climatically constrained time periods,  
40 the main active conduits tend to concentrate at similar elevations, resulting in a distinct cave ‘level’ or still-  
41 stand (Ford and Williams, 2007). Over time, this process leaves a stacked relict cave levels preserved above  
42 the modern active conduit system, creating an inverted passage stratigraphy comparable to that of river  
43 terraces (Sasowsky *et al.*, 1995; Stock *et al.*, 2005).

44 Cave levels can also develop due to lithological heterogeneity. In heterogeneous carbonate sequences such  
45 as the Upper Cretaceous Chalk of northern France, caves may preferentially develop along restricted  
46 stratigraphic discontinuities or ‘inception horizons’ particularly susceptible to dissolution within the  
47 limestone succession (Lowe, 2000). This may occur even in a dynamic situation with river incision followed  
48 by base-level lowering (Palmer, 1987). However, even if passage inception is influenced by lithology,  
49 subsequent passage enlargement either upwards in a phreatic environment or down-cutting in a vadose  
50 system, or due to sediment aggradation, is typically independent of lithology or structure (Filipponi *et al.*,  
51 2009; Sauro *et al.*, 2013).

52 Many studies have related the genesis of relict cave levels and their subsequent abandonment to base-level  
53 dynamics, driven by river incision in fluvial valleys or sea-level oscillations in coastal areas (Piccini and  
54 Landelli 2011; Audra and Palmer, 2013; Calvet *et al.*, 2015; Columbu *et al.*, 2015; Nehme *et al.*, 2016;  
55 Harmand *et al.*, 2017; Pennos *et al.*, 2019; Bella *et al.*, 2019). The rate of river incision is influenced by  
56 several variables. These include climatic forcing, affecting river discharge and sediment transport,  
57 geomorphological evolution as well as geological factors such as lithology, structure and tectonic uplift.  
58 Quaternary climatic variations may increase or reduce discharge, affecting sediment flux in fluvial  
59 catchments, either due to periglacial/glacial processes in high latitudes or increased rainfall in tropical areas,  
60 along with vegetation cover evolution (bio-rhexistasy). This may trigger episodic valley aggradation,  
61 causing hiatuses in base-level lowering, or even base-level rise (Laureano *et al.*, 2016). The latter is most  
62 likely in karst conduit systems developed at or close to the water table adjacent to major rivers (Granger *et*  
63 *al.*, 1991; Constantin *et al.*, 2001).

64 In high-latitude areas where periglacial/glacial processes are the dominant influence on Quaternary valley  
65 incision, climatically-forced incision and aggradation (Aranburu *et al.*, 2014) influences the development  
66 of cave levels. Each phase of fluvial incision and base-level fall increased the hydraulic gradient in the  
67 chalk aquifer, causing a reorganization of the conduit system (Harmand *et al.*, 2017). These respond to  
68 base-level fall by the development of new phreatic conduits graded to the lower base-level, and/or by vadose  
69 incision of the existing passage. The type of response is mainly influenced by local factors (lithology,  
70 fracture density, geological structure) and regional factors such as the magnitude of the base-level fall. In  
71 the Seine valley, the Chalk has a relative high fracture density (0.1-0.3 m fracture spacing), characterized  
72 by frequent regional inception horizons including flint bands, marl seams and hardgrounds, and numerous  
73 closely-spaced vertical to horizontal joints (Duperret *et al.*, 2012; Mortimore, 2018). The availability of  
74 many potential inception horizons and flow pathways coupled with relatively small magnitude falls in base-  
75 level, favors the development of low-gradient, shallow phreatic or epiphreatic conduits close to the

76 contemporaneous base-level rather than a deep vadose incision. The studied caves in the Seine valley are  
77 relatively simple, very low gradient phreatic or epi-phreatic branch-work and maze systems fed by recharge  
78 from the surrounding plateau, often via discrete sinks known locally as *bétoires*, with little documented  
79 vadose development other than shaft drains connecting to the plateau surface. There is no evidence of karst  
80 auto-captures across the meander necks.

81 When defining paleo-water tables from caves, consideration also needs to be given to possible modification  
82 of conduits following the main phase of speleogenesis, which may affect the elevation of the water table  
83 (Audra and Palmer, 2013). This may be due to sediment aggradation during a subsequent cold phase, or  
84 blockage of conduits by external factors (glaciers), or internal collapse or sediment deposition leading to a  
85 reorganization of the conduit network (Skoglund and Lauritzen, 2010). Fortunately, such changes can be  
86 identified from careful interpretation of cave passage morphology. Passage modification due to sediment  
87 aggradation, a process known as cave paragenesis (Renault, 1968) can be identified by several characteristic  
88 features including wall notches, roof pendants, anastomoses channels in roofs and phreatic canyons with  
89 upwards propagating meanders (Lauritzen and Lauritsen, 1995; Pasini, 2009; Farrant and Smart, 2011;  
90 Bella *et al.*, 2019).

91 To investigate the landscape evolution of the Normandy area, each of the relict caves exposed in the Seine  
92 valley was mapped along with detailed geomorphological investigations, passage morphology  
93 characterization and sedimentological observations. Ten speleothems and 144 cave sediment samples were  
94 collected for uranium series and palaeomagnetic dating to determine the minimum age of caves, the timing  
95 of sediment infill and passage abandonment. To create a robust age model constraining the rate of Seine  
96 valley incision, eight cave systems spanning a range of elevations 10-100 m above sea-level (asl) were  
97 dated.

98 By combining a detailed geomorphological assessment of each site with chronological evidence from  
99 uranium series and palaeomagnetic dating, a regional model for cave development in the Chalk was  
100 constructed, linked to the incision of the Seine River. From this, estimates for the rate of valley incision can  
101 be deduced. The estimated incision rate derived from this study is compared to the previously published  
102 incision velocities of the Seine and Somme rivers based on fluvial terrace sequences.

103

#### 104 **Geological setting: The Upper Normandy Plateau and the Seine valley**

105 The Upper Normandy region in northern France (Figure 1A) comprises an extensive plateau developed at  
106 an elevation of ~100-200 m asl. This plateau is deeply incised by the Seine River, a major river system that  
107 drains much of northern France with a catchment area of ~76,000 km<sup>2</sup>. The region has a temperate maritime  
108 climate, with mean monthly temperatures between 3 and 17 °C, and 600-1100 mm precipitation.

109 Around 90% of the studied region is underlain by the Upper Cretaceous Chalk Group, a sequence of flinty  
110 coccolithic limestones up to 300 m thick deposited on the western margin of the Anglo-Paris basin (Lasseur  
111 *et al.*, 2009; Mortimore 2018). The Chalk Group is divided into six formations (Figure 1C), and contain

112 many stratigraphical discontinuities including bands of flint nodules, sheet flints, marl seams, hardgrounds  
113 and sponge beds. These features occur at regular intervals every 0.3-1 m throughout most of the  
114 stratigraphic sequence (Lasseur, *et al.*, 2009; Mortimore, 2018). The frequency of these stratigraphic  
115 discontinuities is much greater in Normandy than in the more basinal parts of the Anglo-Paris basin east of  
116 Dieppe and in southeast England.

117 The Chalk bedrock is typically very gently deformed (e.g. with flexures, low amplitude anticlines),  
118 generally appearing slightly dipping or sub-horizontal, and is locally cut by faults with up to 200 m  
119 horizontal displacement. These typically trend NW-SE (Figure 1C) and were active from the Upper  
120 Cretaceous, when they influenced chalk deposition to the Miocene (Guillocheau *et al.*, 2000; Duperret *et*  
121 *al.*, 2012; Mortimore 2018). Some of these structures were reactivated again in the Pliocene and Quaternary  
122 (Hauchard and Laignel 2008). The Chalk Group is locally overlain by Paleogene sand and clays, and  
123 Pliocene-early Pleistocene marine sands (St-Eustache Fm) and fluvio-marine sands (Lozère Fm) (Lautridou  
124 *et al.*, 1999; Van Vliet-Lanoe *et al.*, 2002) related to the early paleo-Loire-Seine River (Dugué *et al.*, 2009).  
125 Around 90% of the Chalk outcrop is mantled with Quaternary superficial deposits (Laignel *et al.*, 1999),  
126 especially on the plateau surface. These include sand and clay-rich weathering residues ('Clay-with-Flints')  
127 derived from the overlying Palaeogene sediments as well as periglacial deposits. The latter are mainly  
128 represented by Upper Pleistocene loess ('limons des plateaux') up to 5 m thick (Laignel *et al.*, 1999, 2002;  
129 Quesnel, 2003; Antoine *et al.*, 2016), soliflucted deposits, and fluvial terrace deposits.

130

### 131 *Seine valley terraces.*

132 The Seine River has a well-developed sequence of fluvial terraces (Figure 1B), particularly between  
133 Jumièges and Les Andelys (1997; Lautridou, 1983; Lautridou *et al.*, 1999, 2003; Lécolle, 1989; Lefebvre *et*  
134 *al.*, 1994; Antoine *et al.*, 1998, 2000, 2007). These terraces correspond to seven phases of incision and  
135 subsequent aggradation during periglacial cold-stage periods up to ~95 m above the bedrock floor of the  
136 valley. Heights are quoted as Relative Height (RH) based on the elevation above the maximum depth of  
137 fluvial incision (rockhead). In the lower Seine River, up to 16 bedrock-steps were identified (Antoine *et al.*,  
138 2007). The lower level terraces downstream of Rouen are graded to former base-levels below present sea-  
139 level, and are now buried by Holocene marine, estuarine and alluvial sediments. The terraces above 40 m  
140 asl are discontinuous and poorly preserved, and have not been reliably dated (Antoine *et al.*, 2007). In the  
141 neighboring Somme Basin, 100 km to the northeast, up to 10 bed-rock steps from +5-6 to 55 m RH above  
142 the bedrock floor of the valley. Some of these have been dated using a combination of absolute ages and  
143 archeological findings, suggesting that river incision began at *ca.* 1 Ma and incised at an average rate of  
144 0.055-0.060 m·ka<sup>-1</sup> (Antoine *et al.*, 2007).

145 The scale of post-Pliocene uplift and river incision is evident from the widespread occurrence of the middle  
146 Pliocene fluvial Lozère Sand Fm on the plateau surface around Rouen and Le Havre at up to 140 m asl  
147 above the current Seine riverbed (Figure 1B). This sand includes ferromagnesian minerals dated around ~2  
148 Ma (Larue and Etienne, 2000) and marks the former northward course of the palaeo Loire-Seine River into  
149 the English Channel (Tourenq and Pomerol, 1995; Westaway, 2004; Dugué *et al.*, 2009). In the late

150 Pliocene, a marine transgression lead to the deposition of the marine St-Eustache Sand Fm in the coastal  
151 area around Le Havre to the north-west of the study area (Lautridou *et al.*, 1999). A decrease in fluvial  
152 sedimentation in the Seine Valley occurred at this time following diversion of the Loire River to the west.  
153 Since the cessation of marine deposition in the early Pleistocene, the current Seine River has incised into  
154 the Normandy plateau at an average rate of 0.02-0.05 mm·a<sup>-1</sup>, (Guillocheau *et al.*, 2000; Hauchard and  
155 Laignel, 2008).

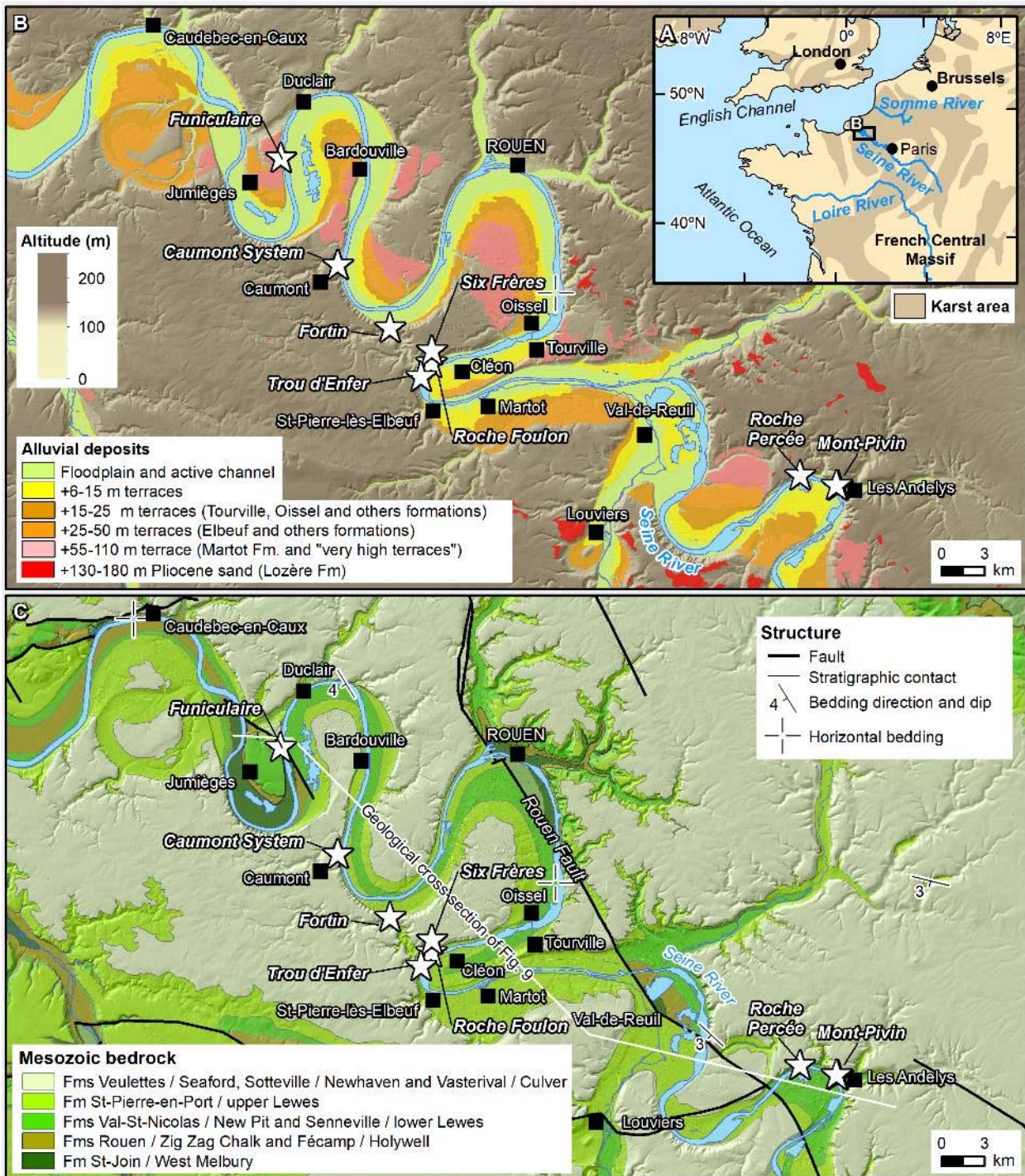
156 In the study area, fluvial deposition began with the development of a suite of ‘very high’ river terraces at  
157 ~92-135 m relative height above maximum incision (RH). These contain unweathered augite crystals  
158 derived from the French Massif Central volcanism (Tourenq and Pomerol, 1995), indicating that the Loire  
159 River still drained into the English Channel. The augite crystals have been dated to *ca.* 1 Ma, implying that  
160 fluvial terraces are Quaternary, but otherwise the chronology is very poorly constrained. Westaway (2004)  
161 assigned these ‘very high’ terraces to between MIS 26-104 (*ca.* 0.98 to 2.6 Ma).

162 The highest well-defined fluvial terrace system, the Martot/Madrillet/Bardouville terrace, is at 70-73 m RH,  
163 correlated with MIS 22 – *ca.* 1.03-0.86 Ma (Westaway 2004). The Martot Fm can be recognized  
164 downstream from Rouen to the Seine Estuary (Figure 1B), but upstream, this formation is not well  
165 preserved. At lower altitude, there are up to three poorly defined terraces at 60-64 m (Rond de France), 50-  
166 54 m, and 38-40 m RH (Antoine *et al.*, 2007). These terraces probably span much of the MIS 23 to 32  
167 (previously Bavelian complex in Lautridou 1983 and Lautridou *et al.*, 1999).

168 At Saint-Pierre-lès-Elbeuf near Rouen (Figure 1B), a fluvial gravel terrace (the Elbeuf Fm) at 30-32 m RH  
169 is overlain by a sequence of loess and with four interglacial palaeosols (Elbeuf I, II, III, IV) (Antoine *et al.*,  
170 2016). OSL dating of the sequence suggests these soils span much of the Middle and Upper Pleistocene  
171 (Cliquet *et al.*, 2009). The Elbeuf I and IV soils have been dated to 164 ± 13 ka and 475 ± 38 ka respectively.  
172 A tufa deposit at the top of the Elbeuf IV soil, dated to *ca.* 400 ka (MIS 11), contains a distinctive *Lyrodiscus*  
173 malacological fauna. An identical fauna occurs in tufa deposits at Vernon, halfway between Rouen and  
174 Paris, which yield uranium series ages equal to or older than 350-400 ka (Lécolle *et al.*, 1989; Rousseau *et*  
175 *al.*, 1992). This characteristic fauna forms a good biostratigraphical marker for MIS 11 and is indicative of  
176 humid and warm forested landscape. A similar tufa at La Celle southeast of Paris yielded a uranium series  
177 age of 388 ka (+/- 69), coeval with MIS 11 (Dabkowski *et al.*, 2012). The uranium series ages give  
178 confidence in the correlation between La Celle and Elbeuf. In both cases, the fluvial terrace underlying the  
179 tufa is attributed to MIS 12.

180 Around 10 m below the Elbeuf terrace another well-defined terrace system, the Oissel Fm, occurs at 22-25  
181 m RH (Figure 1B). This terrace has not been dated. In the Rouen area, the lowest gravel terrace sequence  
182 exposed is the Tourville Fm. The base of this deposit is at 17-18 m RH above the maximum incision of the  
183 Seine River. It comprises a complex sequence (Lautridou *et al.*, 1999) including three gravel units  
184 interbedded with two palaeoestuarine silt beds. These interglacial estuarine deposits, dated by OSL and  
185 ESR (Balescu *et al.*, 1991, 1997) give ages of *ca.* 200 ka (MIS 7) for the upper silt, and *ca.* 300 ka (MIS 9)  
186 for the lower silt. The upper layer contained an exceptional Saalian-age mammal fauna (Lautridou *et al.*,

187 1999). The complex Tourville Fm thus comprises two glacial–interglacial sequences spanning MIS 9 to 6.  
 188 Three further gravel terraces occur stratigraphically below the Tourville Fm (Figure 1B), but as they are  
 189 close the current floodplain and underlie Holocene deposits, they are not well exposed.



190 **Figure 1.** Settings of the study area: (A) Situation of the Upper Normandy in the North of France. (B) Digital Elevation Model of  
 191 the study area (after Institut National de l'Information Géographique et Forestière), showing the position of the eight study caves  
 192 and alluvial deposits (Antoine et al., 2007). (C) Geological map of the Mesozoic bedrock of the study area, after Juignet and Breton,  
 193 (1992), Robaszynski et al. (1998), and Lasseur et al. (2009). Alluvial deposits and geological data are after Bureau de Recherches  
 194 Géologiques et Minières ([www.infoterre.brgm.fr](http://www.infoterre.brgm.fr)).  
 195  
 196

197 **Karst geomorphology**

198 Except for the main Seine River and its tributaries, most of the Normandy plateau is characterized by  
 199 underground drainage within an unconfined karst aquifer. Recharge is predominantly through the Cenozoic

200 semi-permeable superficial formations that cover the plateau (Valdes *et al.*, 2014). These deposits serve to  
201 concentrate surface recharge onto discrete points inducing the formation of deep dissolution pipes. These  
202 are often infilled by reworked surficial sediments, washed in by infiltrating surface water.

203 Over 50 cave systems have been recorded in the Chalk of Upper Normandy, with an aggregate passage  
204 length of over 10 km. The caves are typically segments of relict conduits comprising complex anastomotic  
205 networks that converge into larger galleries (Rodet *et al.*, 2006), although branch-work systems and  
206 divergent conduits are also known (Rodet and Lautridou 2003). The conduits are fed by recharge from the  
207 surrounding plateau, often focused on discrete leakage points (*bétoires*) through the superficial deposits.  
208 Many of the caves are infilled with sand, silt and clay derived from the overlying superficial sediments  
209 (Laignel *et al.*, 2004; Chédeville *et al.*, 2015). Discrete levels of cave development are preserved at  
210 elevations up to ~ 90 m above the present Seine River (Rodet, 1992, 2007). Previous studies (Lautridou,  
211 1983; Lécalle, 1989; Rodet, 1992) correlated these relict cave levels to former base levels in the Seine  
212 valley (Laignel *et al.*, 2003). The only previously published chronological constraint for cave development  
213 is a speleothem in the Caumont cave system at ~13 m asl (21 m RH) dated to  $236 \pm 75$  ka (Rodet, 1992;  
214 Lautridou, 2003).

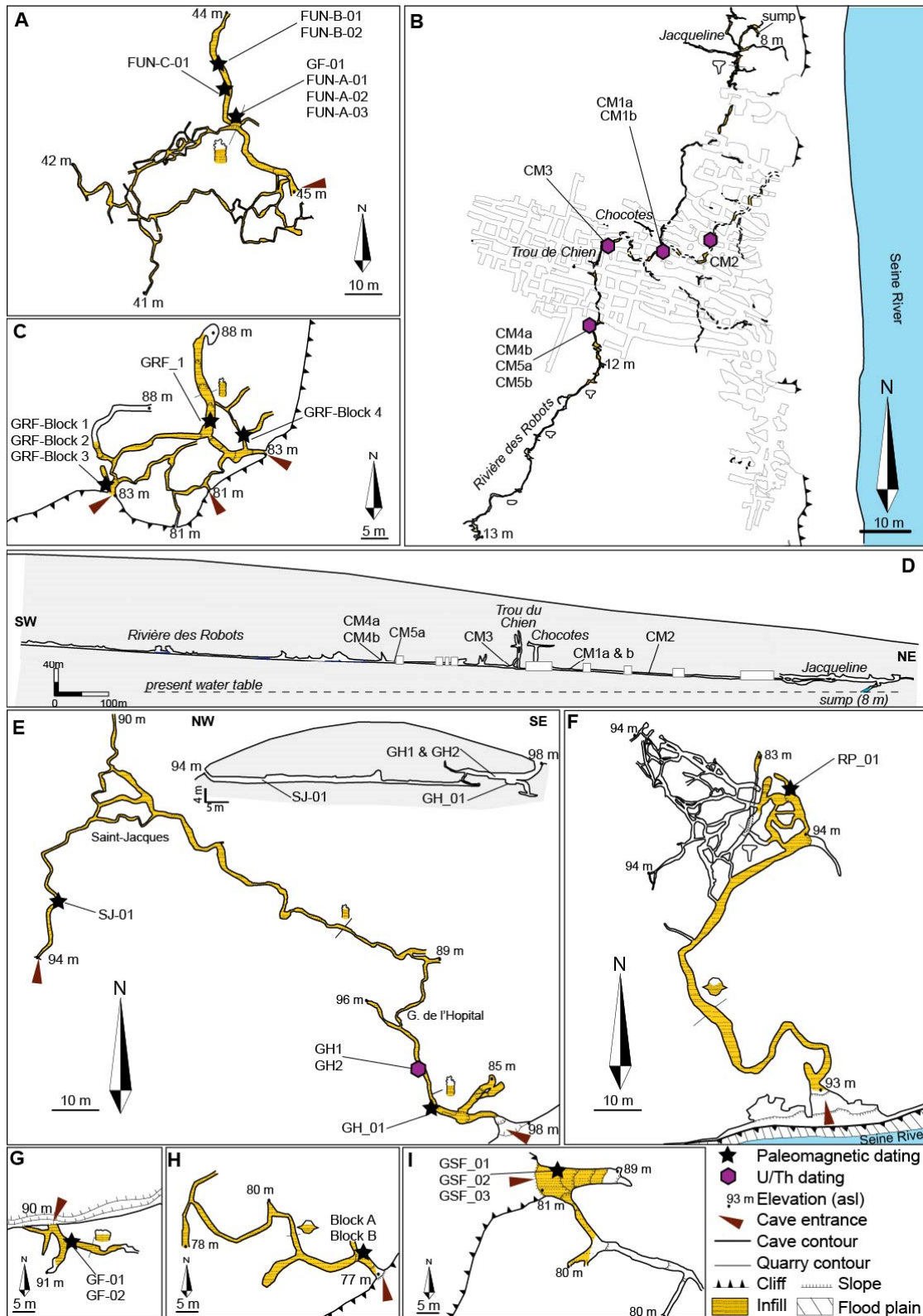
215

### 216 *Study caves*

217 Eight relict and active cave systems in the Seine valley around Rouen were investigated in this study (Figure  
218 1), located between Les Andelys in the southeast to Jumièges in the northwest. These include (Figure 1B)  
219 from the highest to the lowest in relative height above maximum incision (RH), the Mont-Pivin system  
220 (107 m RH) and the neighboring Roche Percée (95 m RH) cave, Fortin (98 m RH), Trou d'Enfer (87 m  
221 RH), Roche Foulon (86-94 m RH), Six Frères (85 m RH), Funiculaire (60 m RH) caves and Caumont active  
222 system (21 m RH).

223 The Mont-Pivin System and Roche Percée caves are located on the north side of the Les Andelys meander  
224 30 km southeast of Rouen (Figure 1B). Both caves, situated at the top of cliffs 80 m above the Seine River,  
225 are relict branchwork systems. The Mont-Pivin system comprises two caves: l'Hôpital (49°14'51.30"N,  
226 1°23'43.66"E, Z: 98 m) and St-Jacques caves (49°14'52.49"N, 1°23'37.88"E, Z: 94 m) that were connected  
227 together by excavating cave deposits that infilled most of the passages (Figure 2G). They have a combined  
228 length of 328 m. Both caves are close to the surface of the plateau and contain well-stratified clay, silt and  
229 sand deposits reworked from the overlying surficial deposits including loess (Rodet, 1992). Vertical shafts  
230 filled with sediment are also present. Prior to excavation, the passage was almost filled to the roof with  
231 sediment. Small flowstone deposits are located along the cave wall and close to the cave ceiling. The Roche  
232 Percée cave (49°15'20.9"N, 1°21'55.3"E, Z: 93 m), located 2.7 km west-northwest of the Mont-Pivin system  
233 (Figure 1B), is 480 m long and comprises a horizontal labyrinthine network of passages (Figure 2H)  
234 partially infilled with interbedded silt, sand and clay deposits and flint nodules. Two vertical shafts  
235 developed along a minor fault have allowed the introduction of loessic material from the plateau above.

236 Fortin cave (49°20'23.8"N, 0°57'47.5"E, Z: 90 m) is located near Moulineaux, 18 km southwest of Rouen  
 237 (Figure 1B). This cave is a small 20 m long branch-work system at an elevation of 98 m RH (Figure 2C).  
 238 The cave is largely sediment choked. An excavated pit reveals more than 1.5 m of interbedded clay, silt and  
 239 very fine sand.



240  
 241  
 242  
 243  
 244  
 Figure 2. The plan view and cross-sections of the studied caves: Funiculaire (A), Caumont (B & D), Roche Foulon (C), Mont-Pivin System (E), Roche Percée (F), Fortin (G), Trou d'Enfer (H) and Six-Frères (I) caves. The sampling of clay-silt for paleomagnetism relative dating and calcite for uranium-series dating are indicated on each cave map. The indicated elevation on each cave map is in meter above sea-level (asl).

245 The Trou d'Enfer and Roche Foulon caves are located at the Cléon meander 15 km south of Rouen (Figure  
246 1B). The Trou d'Enfer (49°18'35.2" N, 0°59'38.4"E, Z: 77 m) is a small relict cave 87 m long at an elevation  
247 of 77 m (Figure 2D). Most of the cave is a network of small passages, with a thick clay-dominated sediment  
248 fill preserved at the entrance. The neighboring Roche Foulon cave (49°19'7.5" N, 1°00'13.1"E, Z: 82-88  
249 m) is a complex network of passages 162 m long, developed on two levels between 86 and 94 m RH,  
250 connected by small sub-vertical to inclined vadose conduits (Figures 2E). Like most other caves, the  
251 passages are largely infilled with clay, silt and sand which have been partially excavated by speleologists  
252 (Chédeville *et al.*, 2015). Over 2 m of sediment is preserved in a section at the southern entrance, with  
253 several other 0.5 to 1 m sections elsewhere in the cave.

254 Six Frères cave (49°14'51.30"N, 1°23'43.66"E, Z: 82 m) is situated on the side of a dry valley near Orival  
255 at an elevation of 86 m RH (Figure 1B). It comprises a large entrance gallery with sediments exposed in  
256 the floor, and a smaller passage leading off, totaling 81 m length (Figure 2F).

257 The entrance of the Funiculaire cave (49°26'39.70"N, 0°51'14.56"E, Z: 45 m) is located on the outer, north  
258 bank of the Jumièges meander, 16 km downstream of Rouen (Figure 1B). The cave is 360 m long and  
259 characterized by a quasi-horizontal labyrinthine network of small relict passages that feed into a single  
260 larger conduit (Figures 2A). The cave is partially infilled by clay and silt with some sand, and flint derived  
261 from passage breakdown, since excavated by speleologists (Coquerel *et al.*, 1993). The sampled section  
262 shown in Figure 4C suggests the main phase of sediment infill was followed by an erosional phase and a  
263 second phase of sedimentation.

264 The Caumont cave system (49°22'41"N, 0°54'47"E, Z: 13 m) is developed on the south bank of the Caumont  
265 meander 25 km southwest of Rouen (Figure 1B). It comprises a branch-work network of passages 4 km  
266 long (Figure 2B) discovered and partially truncated during the excavation of an underground chalk quarry  
267 (Rodet and Lautridou, 2003). The main conduit (lower cave-level) is a 2.4 km long stream passage (Rivière  
268 des Robots) at an elevation of ~13 m asl (21 m RH) (Figure 2B). This stream passage is largely filled with  
269 sediments, predominantly clay silt and sand, capped by speleothem and breakdown deposits. Part of this  
270 sediment fill has been removed by the current stream and by the original explorers, leaving remnants of  
271 speleothem false pavement in parts of the system between the Trou du Chien and Jacqueline passages  
272 (Figure 2B). The downstream end of the stream passage terminates in a sump at 8 m asl (15 m RH) that  
273 connects directly with the Seine River which is tidal at this point. The Trou du Chien and Chocotes galleries  
274 are higher level relict passages situated at an elevation of ~50 m asl (57 m RH; Figure 2B), and accessed  
275 by vertical shafts connecting the two levels.

276

## 277 **Methods**

### 278 *Cave Surveys*

279 Georeferenced cave surveys and geometric parameters were obtained following Ballesteros *et al.* (2015).  
280 Each studied cave was re-surveyed at 1:200 scale using the polygonal cave surveying method with 670  
281 stations and 1431 values of distance, direction and inclination. All measurements were taken using a Disto

282 X2 laser rangefinder. The position of caves entrances was measured using a Garmin GPS (2-3 m precision).  
283 The raw survey data was processed using cave survey software (COMPASS) elaborating the digital  
284 georeferenced cave surveys in ArcGIS (10.3) plotted against topographical and geological maps, aerial  
285 orthophotographs and a digital elevation model (5 m/pixel resolution) of the study area. Four geometric  
286 parameters were calculated from the cave survey database: cave entrance altitudes above sea-level, relative  
287 altitude on the maximum incision of the Seine (RH), length, vertical range and the elevation of the dated  
288 deposits (Table 1).

289

### 290 *Geochronology*

291 Palaeomagnetic dating of fine-grained detrital cave sediments and uranium series dating of speleothem  
292 were used to derive a robust chronology for the cave systems. Both sediments and speleothems necessarily  
293 postdate initial cave genesis, and thus only provide minimal ages for the cave development and later  
294 evolution (Ford *et al.*, 1981; Atkinson and Rowe, 1992). Uranium series (U-Th) dating of calcite speleothem  
295 provides a minimum age for the commencement of vadose conditions within the caves. Palaeomagnetic  
296 dating relies on measuring the magnetic polarity of iron-rich laminated clay and silt deposited in slack  
297 water. Abundant evidence of paragenetic cave development indicates that sediment infill and deposition  
298 was contemporaneous with cave passage formation at or close to fluvial base-level. Other methods used to  
299 date cave deposits such as optically stimulated luminescence (OSL - Ortega *et al.*, 2012) and cosmogenic  
300 burial dating of quartz grains (Anthony and Granger, 2007) were not used in this study due to the lack of  
301 suitable material to date. There was very little suitable quartz material preserved in the caves, despite the  
302 potential for material to have been reworked from the overlying Lozère Fm. Moreover, most caves are  
303 located at shallow depth (<30 m) and thus not suited to cosmogenic burial dating.

304

### 305 *Palaeomagnetism*

306 Palaeomagnetic analysis of cave sediments can provide an important age constraint on the timing of fine  
307 sediment deposition in caves (Sasowsky *et al.*, 1995), especially when different reversals can be identified  
308 in a stratigraphic sequence. Magnetic minerals become oriented toward Earth's magnetic pole during  
309 deposition in still water. Palaeomagnetic dating involves correlating a local magnetostratigraphic column  
310 with the global palaeomagnetic record (Singer, 2014). The chronology of magnetic reversals is well-  
311 established, with the last full reversal, the Matuyama–Brunhes, occurring *ca.* 0.78 Ma (Cande *et al.*, 1995).  
312 The presence of magnetically reversed sediments therefore indicates a minimum age for cave alluviation  
313 of 0.78 Ma. With a stacked series of normal and reversed polarity sediments, this method can be used to  
314 date caves back several million years (Farrant *et al.*, 1995; Stock *et al.*, 2005; Hajna *et al.*, 2010; Rossi *et al.*,  
315 2016; Bella *et al.*, 2019). As a dating tool, palaeomagnetism suffers from two main limitations: first, it  
316 requires suitable fine-grained sediments within the cave, and secondly, it is correlative tool that cannot yield  
317 absolute ages for stratigraphic units except when magnetic reversals are identified and reliably correlated  
318 with the global record. Cave sediment magneto-stratigraphy therefore requires extensive sampling of a

319 sedimentary sequence, backed up with either geomorphological or other age dating evidence to correlate  
 320 any reversals.

321 *Table 1. Elevation of the studied caves (cave entrance altitude, dated deposits' altitude and relative height), geometric parameters (length, vertical*  
 322 *range), with the number of samples for geomagnetic relative dating (total, rejected) and the results of the palaeomagnetic analysis. The deposits*  
 323 *in Caumont cave system were not subject for palaeomagnetic analysis but were dated by uranium series (see table 2)*

| Cave         | Samples Code | Entrance altitude (m asl) | Deposits altitude (m asl) | Relative Height RH (m) | Length (m) | Vertical (m) | Total (n) | Total (n) | Polarity | Magnetic Chronology                                   | Age (Ma)     |
|--------------|--------------|---------------------------|---------------------------|------------------------|------------|--------------|-----------|-----------|----------|---|--------------|
| Mont-Pivin   | MtP          | 94 & 98                   | 90-91                     | 107                    | 328        | 12           | 7         | 0         | N + R    | Matuyama 2 <sup>st</sup> reversal to Jaramillo normal | >1.06        |
| Fortin       | GF           | 90                        | 91                        | 98                     | 46         | 6            | 14        | 1         | R        | Matuyama 2 <sup>nd</sup> reversal                     | >1.06        |
| Roche Percée | RP           | 93                        | 95                        | 95                     | 480        | 18           | 4         | 0         | N        | Jaramillo normal                                      | 0.92 to 1.06 |
| Trou d'Enfer | TE           | 77                        | 79                        | 87                     | 87         | 3            | 9         | 0         | N        | Jaramillo normal                                      | 0.92 to 1.06 |
| Roche Foulon | GRF          | 81-83                     | 82 (Lower)<br>88 (Upper)  | 86<br>94               | 172        | 9            | 36        | 6         | R+ N     | Jaramillo normal to Matuyama 1 <sup>st</sup> reversal | ~ 0.92       |
| Six Frères   | GSF          | 81                        | 82                        | 85                     | 81         | 13           | 16        | 0         | R + N    | Matuyama 2 <sup>st</sup> reversal to Jaramillo normal | ~ 1.06       |
| Funiculaire  | GF-Fun       | 45                        | 42                        | 60                     | 406        | 4            | 45        | 5         | R        | Matuyama 1 <sup>st</sup> reversal                     | 0.78 to 0.92 |
| Caumont      | CM           | 13                        | 15(Lower)<br>50 (Upper)   | 23<br>57               | 4000       | 40           | --        | --        | --       | --  | ---          |

324  
 325 The cave systems exposed in the Seine valley all contain sediments suitable for palaeomagnetic analysis,  
 326 with extensive deposits of laminated clay, silt and fine sand, deposited in slack water setting, co-incident  
 327 with cave development under paragenetic conditions (Farrant and Smart, 2011). An assemblage of 144 clay  
 328 and silt samples was collected from 14 locations in seven caves in the Seine valley near Rouen (Table 1).  
 329 Up to six subsamples were collected from each individual locality, taking samples from different  
 330 stratigraphical levels. Samples were collected using cylindrical orientated cores 25 mm diameter to  
 331 determine magnetic polarities (Table 1). 45 samples were obtained from the Funiculaire cave; 14 from  
 332 Fortin cave; 16 from Six Frères cave; 36 from Roche Foulon cave; nine from Trou d'Enfer cave; seven  
 333 from Mont-Pivin system and four from La Roche Percée cave. Samples were oriented in-situ, using a  
 334 standard magnetic compass. The samples were analyzed using the Geomagnetism Laboratory's RAPID  
 335 system at University of Liverpool, UK (Kirschvink *et al.*, 2008). Each sample was individually step-wise  
 336 demagnetized using alternating field (AF) demagnetization. Each AF demagnetization step randomly  
 337 reorients the magnetic fields of grains with a magnetic coercivity below that of the AF step, effectively  
 338 erasing their net magnetization. The samples were demagnetized from their initial Natural Remnant  
 339 Magnetization (NRM) to a maximum AF field of 100 mT in 10-12 steps, with measurements occurring  
 340 after each step.

341  
 342 *Uranium series dating*

343 <sup>234</sup>U–<sup>230</sup>Th dating was used to complement the palaeomagnetic analyses in caves where old speleothem was  
 344 present. Care was taken to identify older speleothem samples based on appearance and relationship to  
 345 passage morphology and sediments. Samples were collected to constrain a maximum age for the cave  
 346 development within the last normal Brunhes chron. (780 ka to present). Ten samples were extracted from  
 347 the Caumont cave system: seven samples from three flowstone layers and one sample from a speleothem  
 348 growing in small karst voids just above an ancient sediment-filled passage. Two samples were also retrieved

349 in Mont-Pivin system from a thin flowstone layer in the rooftop void capping old fine-grained sediments.  
350 The base of each sample was selected for dating.

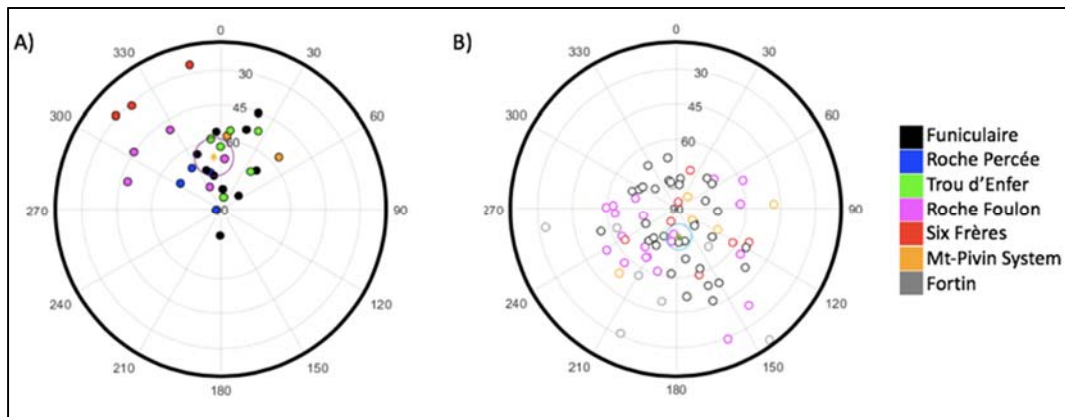
351 Uranium series analyses were conducted at the NERC Isotope Geosciences Laboratories at the British  
352 Geological Survey, Keyworth (UK). Powdered 100 to 400 mg calcite samples were collected with a dental  
353 drill from the base of each sample. Chemical separation and purification of U and Th were performed  
354 following the procedures modified from Edwards *et al.* (1987). Isotopes concentrations were obtained on a  
355 Thermo Neptune Plus multi-collector inductively coupled plasma mass spectrometer (MC-ICP-MS)  
356 following procedures modified from Hellstrom (2006) and Heiss *et al.* (2012). Mass bias and SEM gain for  
357 Th measurements were corrected using an in-house  $^{229}\text{Th}$ – $^{230}\text{Th}$ – $^{232}\text{Th}$  reference solution calibrated against  
358 CRM 112a. Activity ratios are calculated using the decay constants of Cheng *et al.* (2013). Quoted  
359 uncertainties for activity ratios, initial  $^{234}\text{U}/^{238}\text{U}$ , and ages include a *ca.* 0.2% uncertainty calculated from  
360 the combined  $^{236}\text{U}/^{229}\text{Th}$  tracer calibration uncertainty and measurement reproducibility of reference  
361 materials as well as the measured isotope ratio uncertainty. Ages were calculated from time of analysis  
362 (2016) in years before 1950 with a  $2\sigma$  uncertainty error. Many of the samples are contaminated to some  
363 degree by detrital sediment. The effect of detrital contamination was corrected by calculating activity ratios  
364 and dates using a detrital U-Th isotope composition of  $(^{232}\text{Th}/^{238}\text{U}) = 1.2$ ,  $(^{230}\text{Th}/^{238}\text{U}) = 1$  and  $(^{234}\text{U}/^{238}\text{U})$   
365  $= 1$  with  $\pm 50\%$  ( $2\sigma$ ) uncertainties. We consider the impact of detrital Th to be negligible since the  
366  $^{230}\text{Th}/^{232}\text{Th}$  ratio is greater than three. Whilst there are issues with the methods used to correct for the effects  
367 of detrital contamination, the precision of the U-Th method is less critical for landscape evolution modeling  
368 than for palaeoclimate studies. Even with 10% error, the age range of the U-Th method amounts to less  
369 than half a glacial-interglacial cycle, and still can be used to constrain the age of climatically driven  
370 aggradation and incision events.

371

## 372 **Results**

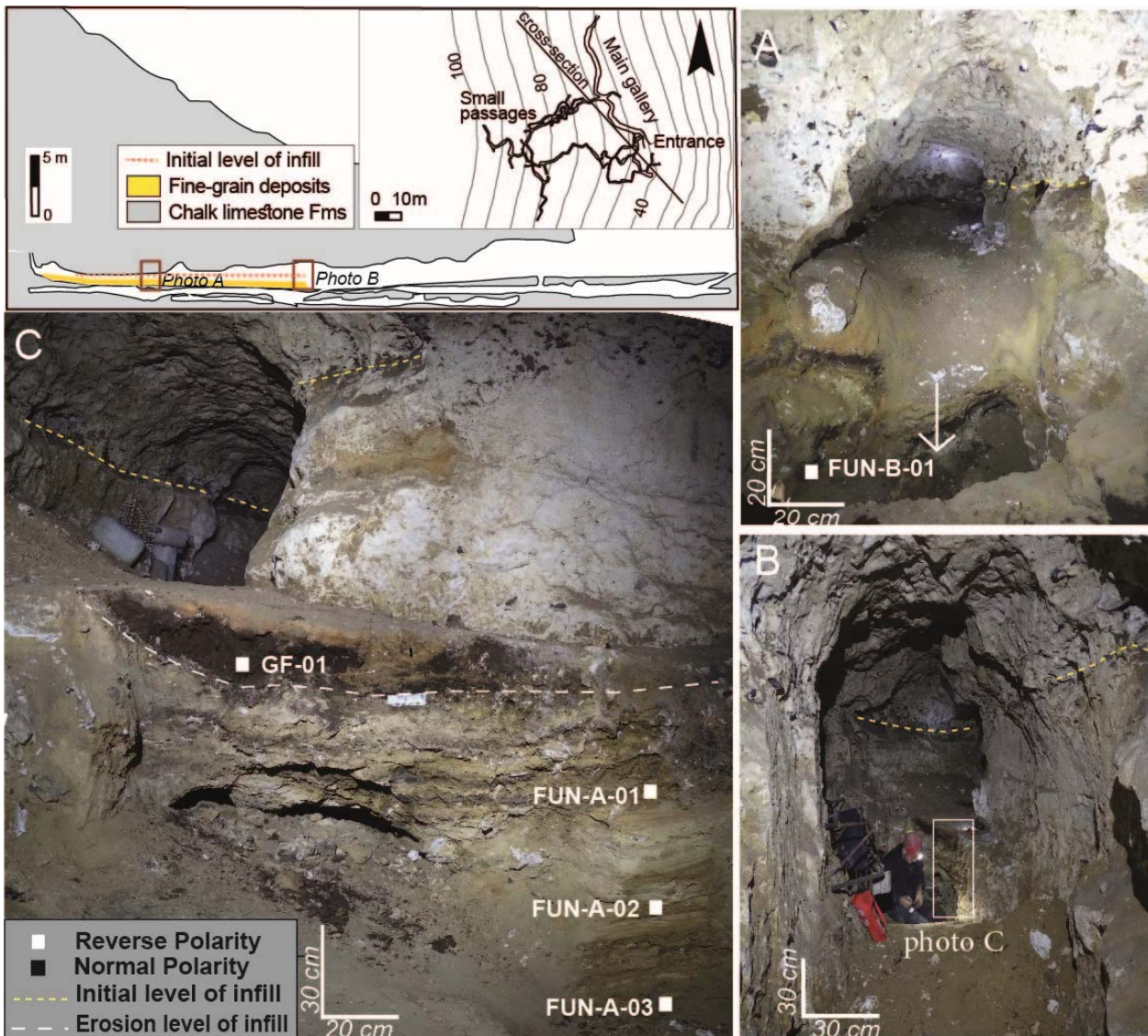
### 373 *Palaeomagnetic relative dating*

374 The results of the palaeomagnetic analyses are given in the supplementary data. Of the 144 samples  
375 obtained, 132 gave useable palaeomagnetic directions (Table 1). Based on reasonable rates of valley  
376 incision and dated river terraces, the lower elevation caves are expected to preserve normal polarity  
377 inclination and declination similar to that at present (Declination:  $0^\circ$ , Inclination:  $64^\circ$ ). Higher elevation  
378 samples are expected to have an antipolar reverse direction. Figure 3 includes the average palaeomagnetic  
379 direction for the samples grouped by inferred polarity. The Normal pole is around  $8^\circ$  shifted from the  
380 modern pole direction. The Reverse pole is  $176^\circ$  offset, which is within error of being antipolar of the  
381 Normal direction. The data present some scatter as the measured sediments are relatively weakly  
382 magnetized. There is little evidence of systematic bias in the direction of the remnant magnetization due to  
383 water flow.



384  
385  
386  
387  
388  
389

**Figure 3.** Equal area stereographic projections of characteristic remnant magnetization (ChRM) directions for all samples. The mean poles are given by solid circles, with the 95% confidence interval given by the corresponding open circle. A) Normal polarity (filled dots) average direction with a declination of 352.4°, inclination of 61.4°,  $\alpha_{95}$  of 10.1° for 30 samples (n). B) Reverse polarity (empty dots) average direction with a declination of 175.5°, inclination of -74.1°,  $\alpha_{95}$  of 7° for 75 samples (n).



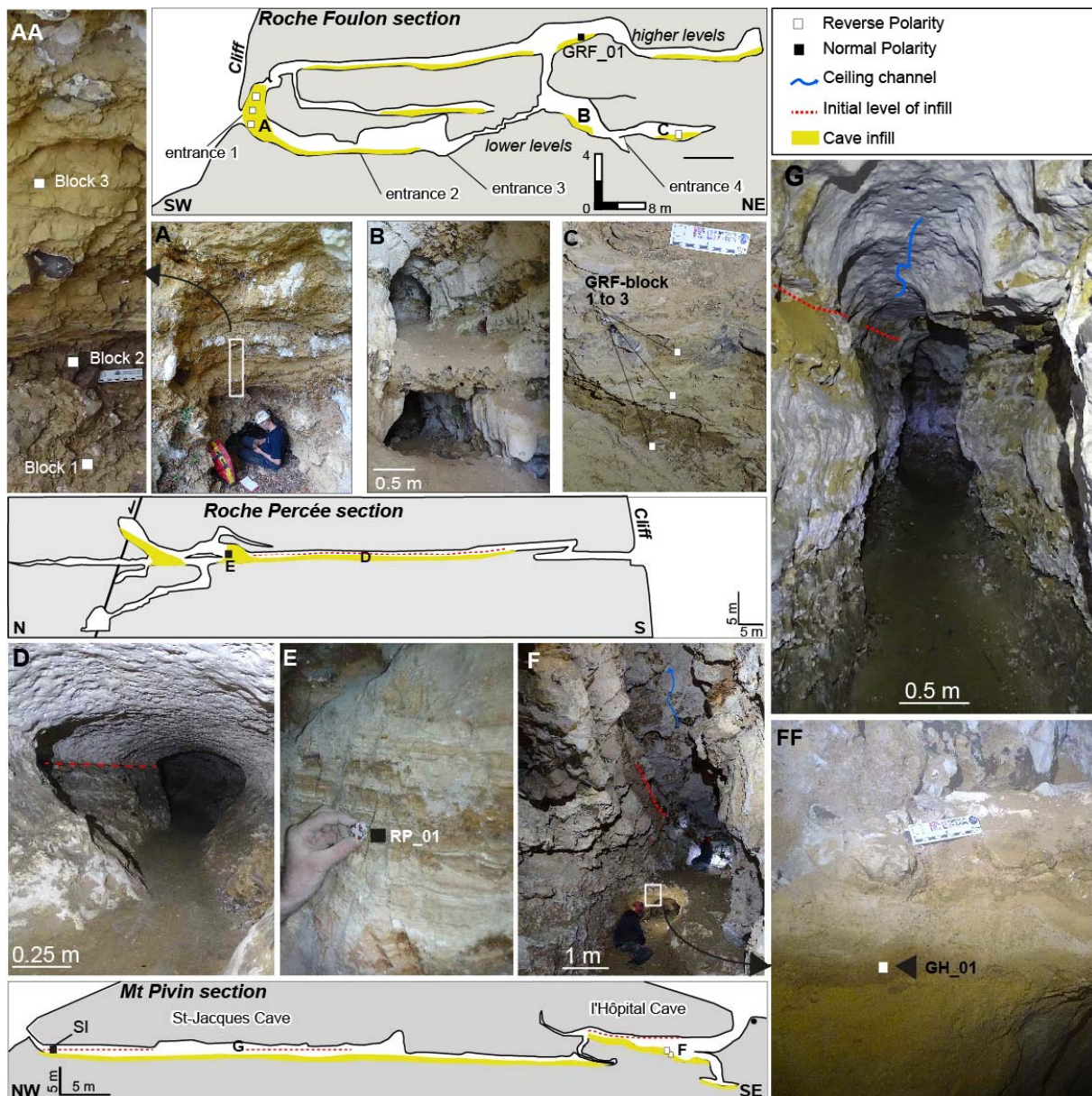
390  
391  
392  
393

**Figure 4.** Passage profile in the Funiculaire cave showing the location of the sampled sections in the Main Gallery. Image A is the location of Section B (looking into the cave). Image B is a view of Section A, with a close up of the section in Image C, both looking into the cave. Note the initial level of infill indicated on A, B and C marked by the yellow dashed line.

394  
395  
396

The lowest level palaeomagnetic samples are from the Funiculaire cave. Three clay and silt layers were sampled from a 1 m sediment section in the main gallery. Here, the palaeo-water table is estimated to be ~60 m relative height (RH) above the base of the maximum incised depth of the Seine River (samples GF-

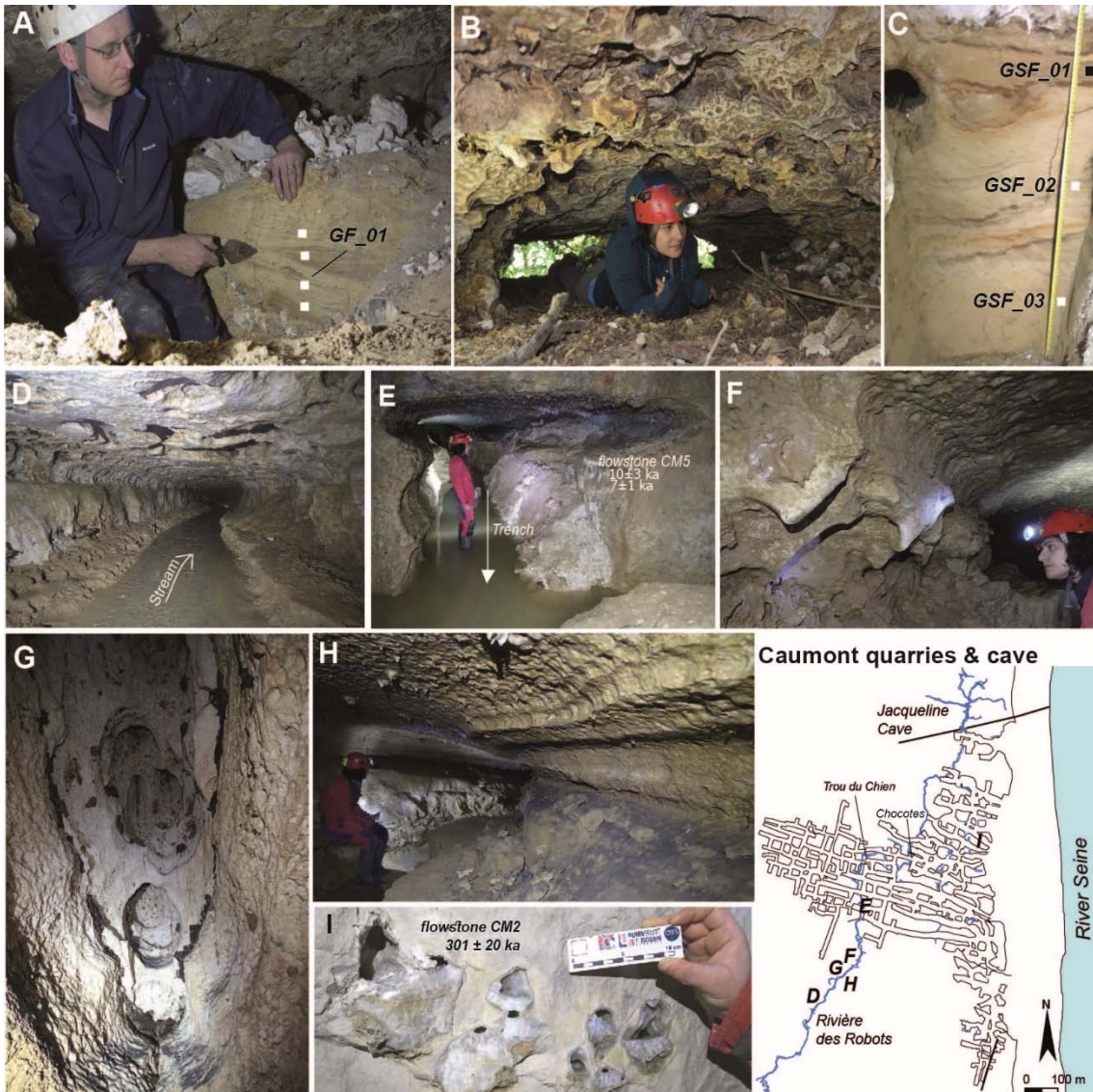
397 1, GF-2, GF-3; Figure 4-A, B and C). All these samples show reverse polarity. Using previous estimates of  
 398 river incision (Guillocheau *et al.*, 2000; Hauchard and Laignel, 2008) these have been ascribed to the  
 399 youngest part of the Matuyama chron.



400  
 401 *Figure 5. Passage sections in the Roche Foulon, Mont-Pivin system and Roche Percée caves with the photos of conduits and*  
 402 *sampld layers in each cave. The sample locations in the Roche Foulon cave section are highlighted in the section, and shown in*  
 403 *the relevant image (A, B and C). The sample site A is shown in more detail in image AA. The Roche Percée cave section and*  
 404 *samples are indicated in images D and E. The Mont-Pivin system sample site is shown in image F, with a more detailed view in*  
 405 *image FF. The St-Jacques cave section is indicated in image G and the sample site (SI) is indicated on the Mt Pivin cross-section.*  
 406 *The level of sediment infill is marked by a red dashed line.*

407 The next lowest cave in the sequence, Roche Foulon, comprises two passage levels between 86 and 94 m  
 408 RH that show more complex results. The lower sediment layers sampled (Figure 5-AA and C) located at  
 409 the more southerly entrance have a reverse polarity (Figure 5), whereas the higher layers (Figure 5-Roche  
 410 Foulon section) located in the upper level (GRF\_1) have a normal polarity. The latter is ascribed to the  
 411 Jaramillo subchron. The passage morphology suggests the sediment fills were deposited within two closely-  
 412 spaced, but separate cave levels, and are thus separated in time (ie higher = older), spanning the end of the  
 413 Jaramillo normal subchron. The samples from the Trou d'Enfer cave at 87 m RH are a similar elevation  
 414 above base-level and also have normal polarity, ascribed to the Jaramillo subchron. Samples from the Six

415 Frères cave at 85 m RH also show a magnetic reversal. The lower layers (GSF\_03 & GSF\_02) have reversed  
 416 polarity whilst the samples from higher in the sequence sediment fill (GSF\_01) record normal polarity and  
 417 are ascribed to the Jaramillo subchron (Figure 6B). Unlike Roche Foulon cave, these samples are from the  
 418 same sediment sequence and record a phase of paragenetic alluviation, and thus the higher samples are  
 419 younger. They record the polarity change at the start of the Jaramillo normal subchron.



420  
 421 **Figure 6.** Sampled deposits and flowstone in Fortin cave, Six Frères cave and the Caumont quarries. A is the section of the sampled  
 422 deposits in Fortin cave. B is the entrance section of Fortin cave showing passage morphology, C is the section sampled in Six  
 423 Frères cave. D to H show the passage morphology in the Rivière des Robots in the Caumont system. I shows flowstone preserved  
 424 in dissolutional pockets associated with relict conduits in Caumont system. The survey shows the location of the images. White  
 425 squares indicate layers with normal polarity and black squares represent layers with reverse polarity.

426 The Roche Percée cave is at a similar elevation above base level (96 m RH) to the Six Frères cave, and  
 427 contain wholly normal polarity sediments from the Jaramillo subchron (Figure 5F). Just upstream, the  
 428 sampled clay and silt layers in the Mont-Pivin system (107 m RH) show reverse polarity, indicating a level  
 429 prior to the start of the Jaramillo subchron at *ca.* 1.068 Ma. Fortin cave at 98 m RH show that three clay  
 430 and silt samples have a reverse polarity (Table 1, Figure 6A), within the latter part of the Matuyama Chron,  
 431 but prior to the Jaramillo subchron.

432  
 433 *Uranium series dating*

434 Eight speleothem samples were collected for uranium series dating from the Caumont cave system, and two  
 435 samples from the Mont-Pivin (l'Hôpital cave) system, from which ten dates were obtained (Table 2). All  
 436 the samples from the Caumont system are younger than ~300 ka. The oldest date,  $301 \pm 20$  ka BP (Figure  
 437 6F) was obtained from a flowstone (sample CM2) lining the inside of an alcove on the wall of a relict  
 438 conduit at ~21-22 m RH. Nearby, a flowstone in the lowest level at site directly below the Chocotes conduit  
 439 (Figure 2D, CM1a and 1b), approximately 2 m lower grew between  $274 \pm 7$  and  $250 \pm 14$  ka BP. A younger  
 440 dated flowstone retrieved in the lowest level of Trou du Chien conduit (Figure 2D; sample CM3) was dated  
 441 to  $127.6 \pm 0.7$  ka BP. Two flowstones were obtained from the 'Rivière des Robots' stream. A stalagmite  
 442 growing on boulders in a vadose rift ~2-3 m above the present stream (CM4a and 4b, Table 2) grew between  
 443  $102 \pm 16$  and  $79 \pm 6$  ka BP. Another speleothem capping a sediment bank 1.2 m above the stream (Figure  
 444 6E; samples CM5a and 5b) grew between  $10 \pm 3$  to  $7 \pm 1$  ka BP.

445 In the Mont-Pivin cave System, two thin flowstone layers deposited between the top of the sediment fill  
 446 (since excavated) and the cave wall and ceiling (Figure 5D) near the l'Hôpital cave entrance give ages  $570$   
 447  $\pm 52$  and  $495 \pm 25$  ka. BP. These much older ages provide a minimum estimate of the timing of passage  
 448 abandonment. However, they are considerably younger than the sediments dated using relative  
 449 palaeomagnetic polarity, implying a significant time gap between sedimentation, abandonment and  
 450 speleothem growth.

451 **Table 2.** Summary of U-Th data from Caumont (CM1 to 5) and Mont-Pivin (GH1 and 2) caves in the Seine Valley. All uncertainties  
 452 are reported at the  $2\sigma$  level. Activity ratios calculated using the decay constants of Cheng *et al.* (2013). 1 – corrected activity ratios  
 453 and dates calculated using a detrital U-Th isotope composition of  $(^{232}\text{Th}/^{238}\text{U}) = 1.2$ ,  $(^{230}\text{Th}/^{238}\text{U}) = 1$  and  $(^{234}\text{U}/^{238}\text{U}) = 1$  with  $\pm$   
 454 50% ( $2\sigma$ ) uncertainties. 2 – uncertainty includes 0.2% external reproducibility. 3 – uncertainty includes 0.1% external  
 455 reproducibility.

| Cave name                  | Sample ID | $^{238}\text{U}$ (ppm) | $^{232}\text{Th}$ (ppm) | $(^{230}\text{Th}/^{232}\text{Th})$<br>measured | $(^{230}\text{Th}/^{234}\text{U})$<br>Corrected <sup>1,2</sup> | $(^{234}\text{U}/^{238}\text{U})$<br>Corrected <sup>1,3</sup> | $\rho_{08-48}$ | Age un-corrected<br>(ka) | Age corrected<br>(ka BP) <sup>1</sup> | $(^{234}\text{U}/^{238}\text{U})$<br>initial |
|----------------------------|-----------|------------------------|-------------------------|---|--|---|----------------|--------------------------|---------------------------------------|--|
| <b>Caumont lower level</b> |           |                        |                         |   |  |   |                |                          |                                       |  |
| Chocotes &                 | CM2       | 0.07                   | 0.063                   | 3.52  | $1.2 \pm 0.1$  | $1.18 \pm 0.08$   | 0.99           | $325 \pm 8$              | <b><math>301 \pm 20</math></b>        | $1.4 \pm 0.2$                                |
| Trou du                    | CM1b top  | 0.08                   | 0.065                   | 4.49  | $1.18 \pm 0.09$  | $1.24 \pm 0.07$   | 0.97           | $268 \pm 4$              | <b><math>250 \pm 14</math></b>        | $1.5 \pm 0.2$                                |
| Chien lower                | CM1a base | 0.04                   | 0.014                   | 9.46  | $1.25 \pm 0.04$  | $1.28 \pm 0.03$   | 0.98           | $282 \pm 4$              | <b><math>274 \pm 7</math></b>         | $1.59 \pm 0.07$                              |
| levels                     | CM3       | 0.11                   | 0.001                   | 178.8   | $0.793 \pm 0.002$  | $1.129 \pm 0.002$   | 0.38           | $128.0 \pm 0.6$          | <b><math>127.6 \pm 0.7</math></b>     | $1.185 \pm 0.003$                            |
| Robots                     | CM4b top  | 0.54                   | 0.152                   | 6.34  | $0.55 \pm 0.04$  | $1.07 \pm 0.03$   | 0.71           | $86.8 \pm 0.4$           | <b><math>79 \pm 6</math></b>          | $1.08 \pm 0.04$                              |
| stream                     | CM4a base | 0.15                   | 0.106                   | 3.27  | $0.7 \pm 0.1$  | $1.11 \pm 0.09$   | 0.78           | $122.8 \pm 0.7$          | <b><math>102 \pm 16</math></b>        | $1.2 \pm 0.1$                                |
|                            | CM5a top  | 0.3                    | 0.016                   | 4.66  | $0.07 \pm 0.01$  | $1.094 \pm 0.007$   | 0.32           | $8.43 \pm 0.03$          | <b><math>7 \pm 1</math></b>           | $1.096 \pm 0.008$                            |
|                            | CM5b base | 0.24                   | 0.031                   | 3   | $0.10 \pm 0.02$  | $1.08 \pm 0.02$   | 0.35           | $13.81 \pm 0.05$         | <b><math>10 \pm 3</math></b>          | $1.08 \pm 0.01$                              |
| <b>Mt-Pivin system</b>     |           |                        |                         |   |  |   |                |                          |                                       |  |
| G. Hôpital                 | GH2       | 0.17                   | 0.002                   | 332.92  | $1.041 \pm 0.002$  | $1.037 \pm 0.001$   | 0.05           | $495 \pm 25$             | <b><math>495 \pm 25</math></b>        | $1.151 \pm 0.009$                            |
|                            | GH1       | 0.13                   | 0.007                   | 64.15   | $1.058 \pm 0.003$  | $1.045 \pm 0.002$   | 0.45           | $571 \pm 52$             | <b><math>570 \pm 52</math></b>        | $1.22 \pm 0.03$                              |

## 457 Discussion

### 458 *A model of speleogenesis in a fluvial context*

459 Groundwater flow and cave development in the Chalk aquifer is intrinsically linked to river incision by the  
 460 Seine River which forms the regional base-level, and climatic variability. The Quaternary evolution of the  
 461 Seine valley is driven by glacial-interglacial climatic variations, with active incision interspersed with  
 462 phases of fluvial gravel aggradation. These cycles of incision and aggradation are superimposed on regional  
 463 scale Plio-Quaternary uplift leading to the sequential development of cave levels and river terraces. Dating  
 464 of the terrace deposits in the Seine and the Somme basins (Lautridou *et al.* 2003; Antoine *et al.*, 2007)  
 465 suggested that each terrace represents generally a single glacial-interglacial cycle. Models of terrace

466 formation propose that each cycle is characterized by short period of bedrock incision during the transition  
467 from a temperate to a (peri)glacial climate (Antoine *et al.*, 2007), followed (with a variable lag time lag,  
468 Tofelde *et al.*, 2019) by a phase of gravel aggradation (Bridgland, 2000; Bridgland and Maddy, 2002) as  
469 sediment liberated during the climatic deterioration phase feeds into the major river systems. These periods  
470 of climate driven incision, sediment production and ensuing gravel aggradation influenced conduit systems  
471 in the adjacent aquifer, both in their initial development but also subsequent evolution of the system.

472 A sequential model of conduit inception, enlargement, paragenetic modification and abandonment is  
473 proposed. Initial conduit development occurred following fluvial incision and base-level lowering at the  
474 onset of a glacial episode. Cave passage morphology indicates these were low gradient systems developed  
475 under phreatic or epiphreatic conditions at shallow depths (<10 m) beneath the contemporary water table.  
476 These are typically developed on one of the many potential inception horizons present in the Chalk  
477 sequence. Which inception horizon is utilized depends on its geometry and position relative to the local  
478 base-level. A complicating factor is the time needed to develop karstic conduits. Geomorphological  
479 response times can lag behind changes in environmental parameters (Tofelde *et al.*, 2019). The time  
480 required for conduit development from inception to a passage c. 1 m in diameter is  $\sim 10^3$  -  $10^4$  years.  
481 Consequently, new conduit systems initiated during the transition from warm to cold climate and graded to  
482 the new lower River Seine base-level are typically not developed enough to take all the flow before  
483 groundwater circulation is curtailed during the peak of the subsequent glaciation. Consequently many of  
484 existing conduits systems were still active, at least during periods of high flow, for a considerable time after  
485 base-level fall whilst the lower level conduits continued to enlarge.

486 In the later stages of the transition from a temperate to a glacial climate, a decrease in surface vegetation  
487 and increased erosion and sinkhole collapse led to periodic influxes of sand, silt and clay into the aquifer.  
488 These sediments, derived from the overlying Clay-with-Flints, loessic deposits and the Lozère Fm  
489 (Chédeville *et al.*, 2015), often infilled existing cave passages, forcing further dissolutional enlargement  
490 upwards towards the water table. This process left distinctive paragenetic features on the cave walls and  
491 ceiling. These include pendants and half tubes, anastomoses, 'drainage grooves' (Palmer, 2007), bedrock  
492 fins, notches, flat solutional ceilings ('laudecke'), and paragenetic solution ramps (Farrant and Smart,  
493 2011). The latter feature, also termed 'oblique limit benches' (Jaillet *et al.*, 2011) form below the water-  
494 table by lateral dissolution just above the sediment fill, and may be horizontal, inclined or undulating,  
495 depending on the nature of the sediment surface. Notches can also form in vadose environments by lateral  
496 erosion by a stream flowing over a sediment fill.

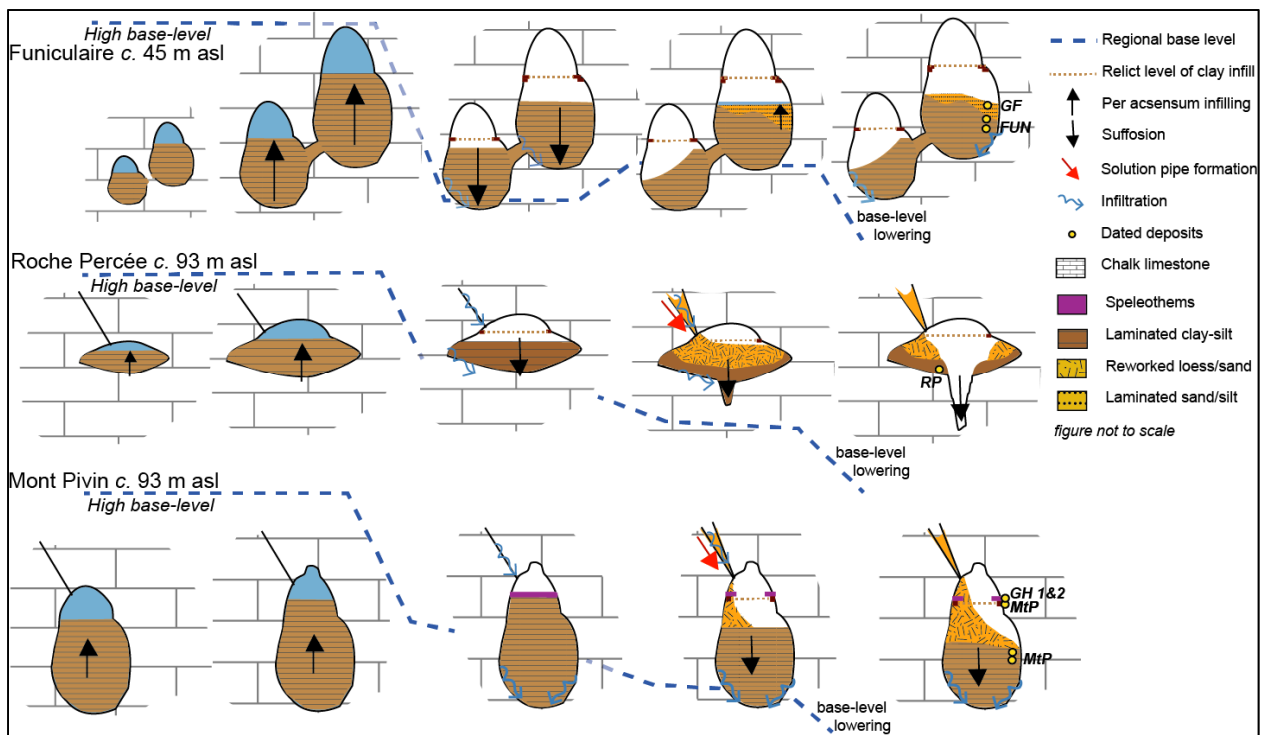
497 Paragenetic development led to the development of complex sedimentary fills, with multiple phases of  
498 sediment injection, deposition and erosion. The low discharge and shallow gradients of most of the conduits  
499 studied, coupled with the predominance of clay, silt and fine sand from the overlying superficial deposits  
500 favoured the deposition of fine-grained sediments in a low-energy environment. Climatic fluctuations drove  
501 the periodic influx of sediment followed by long periods of quiescence and ponding. Localized breakdown  
502 and collapse generated more angular, coarser breccias with chalk and flint clasts. Continued upwards

503 dissolution reduced the hydraulic flux and generated the accommodation space for continued sediment  
504 accumulation. In this way, stacked sequences of locally cross-bedded loessic silts and fine sands,  
505 interbedded with laminated silty clay and localized chalk & flint breccias accumulated.

506 During peak glacial events, groundwater circulation was largely curtailed and sediment influx reduced.  
507 Renewed groundwater circulation in the subsequent interglacial led to the continued enlargement of the  
508 immature conduits initiated during the pre-glacial phase of base-level fall. This enabled the water-table to  
509 fall to the level of the previous terrace aggradation. As these lower conduits enlarged, the older, now largely  
510 sediment filled higher level conduits became defunct. Some modification of these older relict conduits by  
511 invasive vadose inlets led to localized washing out of sediment and the development of vadose trenches  
512 and shafts.

513 The combined result of aggradation and incision of the Seine River is a stacked suite of relict quasi-  
514 horizontal phreatic conduit systems at discrete levels, each developed at or just below the contemporaneous  
515 water table in a shallow phreatic zone. Models of terrace and cave formation suggest that although each  
516 relict cave level reached maturity during interglacial conditions, they are graded to the level of sediment  
517 aggradation from the preceding cold phase (Bridgland and Maddy, 2002; Häuselmann *et al.*, 2008), and  
518 thus can be linked to terrace levels. Dating of sediments and speleothem deposits within these relict cave  
519 systems gives a minimum age for passage abandonment and hence base-level fall. Comparing the altitude  
520 and age of alluvial river terraces with dated cave levels can help constrain rates of river incision and the  
521 evolution of the karst system.

522 Figure 7 shows conceptual model scenarios for karst conduit development in the Seine Valley, using three  
523 representative caves as references. In the Funiculaire cave (Figure 7), paragenetic features including half  
524 tubes, pendants and anastomotic channels (Farrant and Smart, 2011) suggest the cavity was partially infilled  
525 when the cave was still an active conduit (Figure 4), leaving an open phreatic tube above the sediment fill.  
526 Many small, largely sediment filled paragenetic conduits feed up into a larger horizontal passage with an  
527 open phreatic tube above the sediment fill and scallops indicating flow to the south. The passage  
528 morphology suggests that sediments were deposited under shallow phreatic or epiphreatic conditions,  
529 probably at or close to the level of the water-table. Localized chalk and flint breccias indicate localized  
530 breakdown when the conduit was active. Later erosion and sediment compaction following base-level fall  
531 led to the partial removal and reworking of the sediment fill. Similar features are observed in Fortin cave  
532 with paragenetic half-tubes, anastomoses and abundant scalloping on the ceiling (Figure 6). Other caves  
533 such as Roche Foulon (Figure 5D) and Mt-Pivin (Figure 5F and G) show half tubes and large scallops on  
534 the ceiling with sediment infill levels reaching the cave ceiling.



535  
536  
537  
538

**Figure 7.** Synoptic model for the evolution of the studied caves along the Seine valley. The development stages for each cave run separately from left to right. The yellow circles refer to dated deposits (Palaeomagnetic sample) and dated speleothems (uranium series). The dated samples are referred with their codes in Table 1 and 2.

539  
540  
541  
542  
543  
544  
545

The Roche Percée system provides a slightly different model of conduit development. Initial phreatic enlargement and localized minor paragenetic modification was followed by passage abandonment. Late stage invasive vadose inflows via shaft drains cut vadose trenches and shafts, documenting continued readjustment to base-level lowering along with sediment evacuation (Figure 7). By contrast, the Mont Pivin system, initial phreatic development followed by paragenetic enlargement created a sediment filled canyon. Following passage abandonment, speleothem deposits were able to grow over detrital infill. Later invasive influxes of sediment and water entering via shaft drains removed and redeposited some of the sediment.

546  
547  
548  
549  
550  
551  
552  
553  
554  
555

The Caumont system also displays clear evidence of paragenetic development. The present conduit (Rivière des Robots) is a c. 2 m deep paragenetic canyon with localized roof pendants (Figure 6F) and a wider solutional notch at roof level, creating a flat ‘laudecke’ ceiling above the sediment fill (Figure 6D and H). This epi-phreatic notch marks the water-table prior to base-level fall. Several high-level rifts attest to an earlier phase of phreatic development (Figure 6G). Much of the sediment has been recently flushed out by the stream following breaching of the conduit by the quarry, aided by the early explorers, revealing the canyon form. Small speleothem deposits occur on top of the sediment fill indicating the epi-phreatic zone, and have been left as “false floors” (ancient pavement) after the sediment was removed. These morphological observations coupled with the sediment infill indicate that most of the cave passages were formed under paragenetic conditions with sedimentation occurring when the cave conduit was functioning.

556

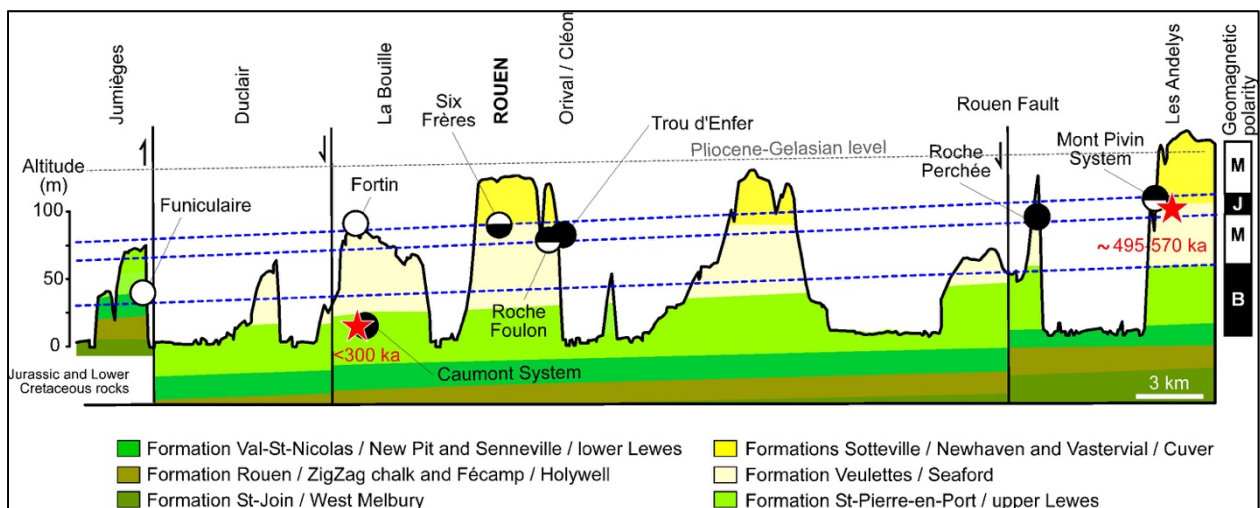
### *Landscape evolution model of the Seine valley*

557  
558  
559

Figure 8 displays the reconstructed paleo-water table in the Seine Valley for the last million years, showing regional levels inclined at *ca.* 0.06% toward the Seine estuary which represents the current base-level. This represents the foreshortened gradient across the meanders rather than the actual river gradient. The highest

560 and therefore oldest cave system in the Seine valley is the Mont-Pivin system formed when the water table  
 561 was at or higher than ~107 m RH. Both this and Fortin cave probably predate the Jaramillo subchron, so  
 562 these cavities are likely to be older than 1.071 Ma. These most likely developed during MIS 33 or 35 and  
 563 were infilled at the onset of the following glacial phase. The commencement of the Jaramillo subchron is  
 564 recorded by the sediments in the Six Frères cave, which was probably active during MIS 31. Later, three  
 565 cave systems were developed during the Jaramillo subchron. The Trou d'Enfer, Roche Foulon (upper part)  
 566 and Roche Percée caves contain sediments deposited during the Jaramillo subchron between 1071 and 990  
 567 ka, suggesting the caves developed during MIS 27 or 29. Although the Roche Foulon (upper) and Roche  
 568 Percée caves are at different elevation above sea-level, they are at similar relative elevation (70-80 m) above  
 569 the Seine River, indicating that they are coeval. The transition back to reversed polarity sediments is  
 570 recorded in the lower part of Roche Foulon cave (MIS 25). The Funiculaire cave (Figure 7) was active  
 571 during the late Matuyama Chron, probably during MIS 21 at around 860 ka.

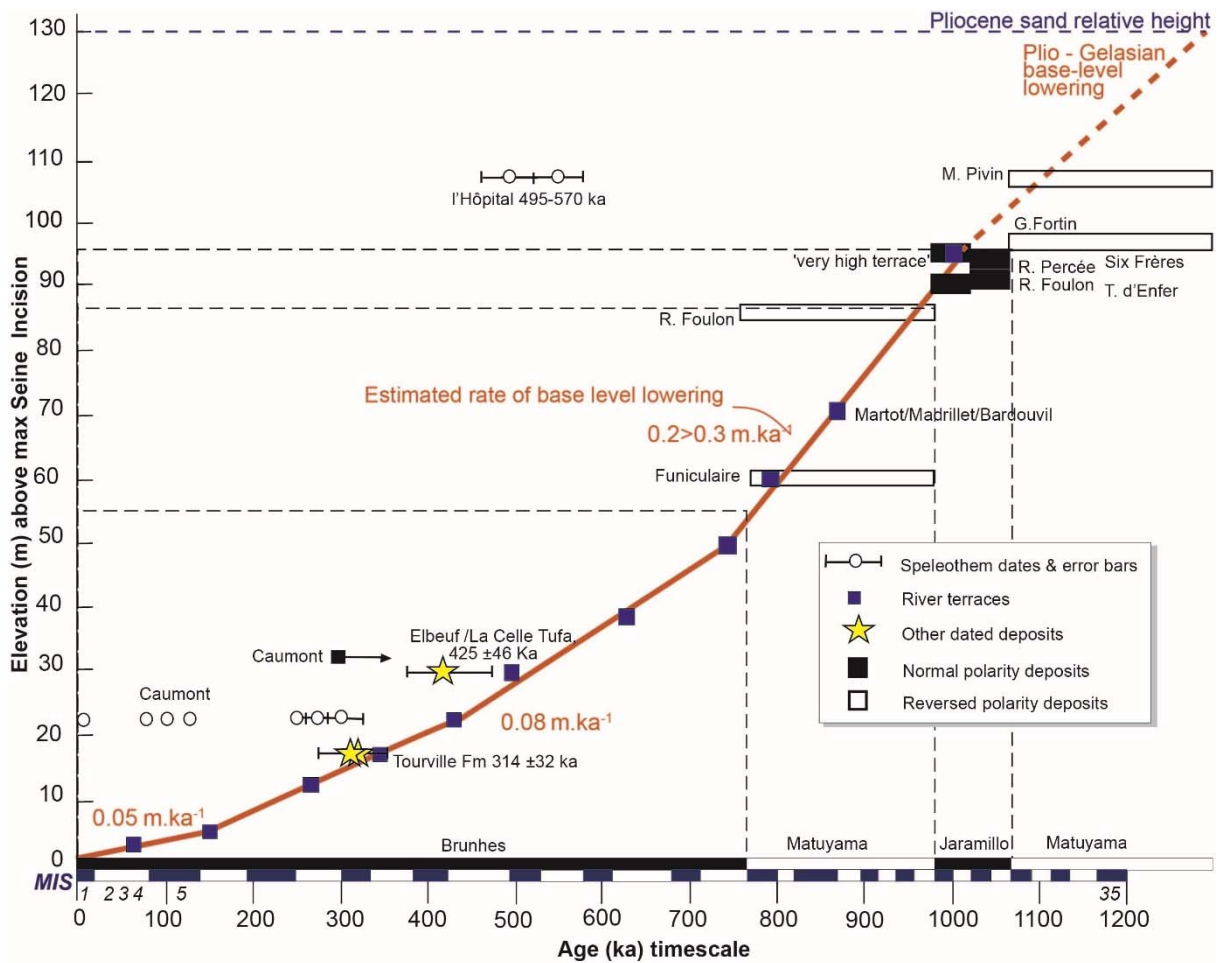
572 The lowest cave level is the Caumont cave system. Here, an initial system of phreatic conduits developed  
 573 when the water table was higher than ~57 m RH. Following based-level fall, a lower level conduit system  
 574 developed at ~21 m RH (Figure 2- Caumont section). The system has now been partially drained.  
 575 Speleothem deposits overlying sediments and debris falls in the lower levels dated to  $274 \pm 7$  ka imply that  
 576 the upper cave level was drained prior to MIS 7. By implication, this shows the Caumont caves system has  
 577 been active for >300 ka, and the water table was at or below 23 m RH during MIS 7 and 5 (Figure 9).  
 578 Fluvial aggradation in the lower Seine valley driven by a marine high stand during the last interglacial stage  
 579 did not affect the Caumont cave system, as active speleothem growth was occurring at this time.



580  
 581 **Figure 8.** Synthetic stratigraphical log for the middle section of the lower Seine Valley with the relative height of the studied caves,  
 582 the projection of the palaeo-water table gradients. The palaeo-magnetic relative dating of the sediment infilling is marked in white  
 583 (inverse) and black (normal) circles and the U-Th dating of speleothem representing the abandonment of the caves by the regional  
 584 drainage system, are marked in red stars. The altitude (vertical axis) of the log is exaggerated.  
 585

586 The dating evidence from the cave systems, after accounting for the gradient of the Seine valley, suggests  
 587 they can be correlated with the dated alluvial terrace sequences (Figure 9). The results from the dating  
 588 indicate most of the higher-level cave systems predate the development of most of the well-preserved  
 589 terrace sequences and suggests that incision began before *ca.* 1.1 Ma. The onset of valley incision is  
 590 constrained by the presence of late Pliocene marine sand (St-Eustache Fm) and the La Londe clay of

591 Gelasian age (1.8-2.58 Ma) on the Upper Normandy plateau (Van Vliet-Lanoe *et al.*, 2002). The highest-  
 592 level cave systems probably developed around MIS 33 or 35, just prior to the deposition of the highest  
 593 terraces at ~95 m RH (Figure 9), and may be attributed to the palaeo-Seine-Loire river catchment (Westway,  
 594 2004).



595 **Figure 9.** Estimates of the incision rates for the Seine valley from fluvial terraces and tufa deposits and caves (speleothems and  
 596 sediment deposits- this study). The terraces positions are based on their elevation above maximum incision (Present relative height  
 597 - Base-level above Seine bedrock) as well as on dating performed on fluvial sediments and tufas from previous studies (Lautridou  
 598 *et al.*, 1999, Antoine *et al.*, 2000, 2007, Cliquet *et al.*, 2009) for Rouen, Oissel, Tourville and St-Pierre les Elbeuf-la Celle Fm. The  
 599 Martot/Bardouville/Madrillet and Rond de France are less-well dated but correlate with other dated terraces (Westway *et al.*,  
 600 2004; Lautridou *et al.*, 1999, Antoine *et al.*, 2007). The 'very high terraces' with an average RH (Antoine *et al.*, 2007) dated to  
 601 about 1 Ma (Tourenq et Pomerol, 1995) define the onset of the River Seine incision after separation from the Loire Basin. The  
 602 black square with an arrow for Caumont presumes a speleogenesis onset of this karst system earlier than ca. 300 ka.  
 603

604 The dating of the various cave levels, coupled with estimated ages of fluvial terraces and cave levels based  
 605 on correlations with marine isotope curves enable rates of river incision to be calculated (Figure 9).  
 606 Magnetic polarity data suggests there has been ~58-60 m of incision since Brunhes-Matuyama transition,  
 607 implying an average rate of river incision of 0.074-0.076 m·ka<sup>-1</sup> over this time, and up to 90 m since the  
 608 start of the Jaramillo subchron (equivalent to an average of ~0.084 m·ka<sup>-1</sup>). The evidence from the cave and  
 609 terrace sequences indicate that river incision was initially slow during the early Pleistocene, followed by a  
 610 phase of more rapid river incision from MIS 28 to 19 (ca. 1 to 0.7 Ma), with rates reaching a maximum of  
 611 ~ 0.30 m·ka<sup>-1</sup>. This phase was probably triggered by the incision of the English Channel River (Gibbard  
 612 and Cohen, 2015) and matches the onset of widespread erosion within the Paris Basin (Guillocheau *et al.*,  
 613 2000; Lagarde *et al.*, 2000; Robin *et al.*, 2003). Bridgland and Westaway (2008) suggest there was a global  
 614 acceleration of uplift at the time of, and perhaps in response to, the Mid-Pleistocene Revolution. Later,

615 incision rates dropped to  $\sim 0.08 \text{ m}\cdot\text{ka}^{-1}$  from MIS 19 to 5 (Middle Pleistocene), and  $0.05 \text{ m}\cdot\text{ka}^{-1}$  from MIS  
616 5 to present-time (Upper Pleistocene).

617 Obtained rates are comparable with rates estimated by Lagarde *et al.*, (2000) and Westaway (2004). Antoine  
618 *et al.* (2000) derived average rates of  $0.055\text{--}0.060 \text{ m}\cdot\text{ka}^{-1}$  since the end of the MIS 19 from the fluvial terrace  
619 sequences. Pedoja *et al.*, (2018) reported apparent uplift rates of  $0.04 \pm 0.01 \text{ mm}\cdot\text{a}^{-1}$  since MIS 5e ( $\sim 122 \pm$   
620  $6 \text{ ka}$ ), and mean Middle Pleistocene eustasy-corrected uplift rates of  $0.09 \pm 0.03 \text{ mm}\cdot\text{a}^{-1}$  from marine  
621 terraces on the Cotentin Peninsula northwest of the Seine valley. The latter are similar to the rates derived  
622 from this study. The similitude between the marine, fluvial terraces and cave data suggests that incision of  
623 the Seine River is controlled by gradual long-term tectonic uplift of the region, superimposed by shorter  
624 timescale eustatic variations, rather than localized variable incision. There is little evidence from the data  
625 of any impact of the catastrophic breaching of the Dover-Artois ridge and opening of the Dover Strait during  
626 the Elsterian–Anglian glaciation (Gupta *et al.*, 2017).

627

## 628 **Conclusion**

629 Stacked sequences of relict cave levels, combined with river terraces can provide valuable quantitative  
630 evidence for landscape change during the Quaternary. This example from the lower Seine valley  
631 demonstrates multiple phases of phreatic groundwater circulation and conduit development linked to  
632 progressive river incision. These cave levels were graded to contemporaneous base-levels dictated by the  
633 incision of the Seine River and can be correlated with fluvial terrace sequences. The evolution of the conduit  
634 systems is influenced by climatic changes during the Quaternary. Dating of detrital deposits and  
635 speleothems preserved within these caves enables the timing of cave development, and hence fluvial  
636 incision to be constrained, particularly during MIS 28-19 when the fluvial terrace record is poorly  
637 constrained. Paleo-magnetic dating of sediment infills indicate that the highest-level caves were formed  
638 and being actively infilled prior to the start of the Jaramillo subchron at 1.068 Ma, probably in relation to  
639 the ancient Seine-Loire River. The evidence from the cave and terrace sequences suggest incision was  
640 initially slow during the early part of the Pleistocene, but accelerated from MIS 28 to 19 (*ca.* 1 to 0.7 Ma),  
641 with rates reaching a maximum of  $\sim 0.30 \text{ m}\cdot\text{ka}^{-1}$ , dropping to  $\sim 0.08 \text{ mm}\cdot\text{ka}^{-1}$  from MIS 19 to 5 (Middle  
642 Pleistocene; *ca.* 0.78-0.12 Ma), and  $0.05 \text{ m}\cdot\text{ka}^{-1}$  from MIS 5 to present-time (Upper Pleistocene). This  
643 approach can be used in other karst regions and is particularly valuable where the river terrace record is  
644 absent or fragmentary.

645

## 646 **Acknowledgements**

647 This work was funded by the Institut de Recherches Interdisciplinaire Homme-Société (University of  
648 Rouen-Normandy). Financial support for laboratory analysis and uranium series dating was provided by  
649 the UK Natural Environment Research Council (NERC). Dr. Mark Woods (British Geological Survey) is  
650 acknowledged for his involvement during field trips. We would like to thank all speleologists from the

651 Comité Régional de Spéléologie de la Fédération Française de Spéléologie and the Centre Normand  
652 d'Étude du Karst for their fieldwork involvement and their help to provide maps for the studied caves.  
653 Farrant and Sahy publish with the approval of the Executive Director, British Geological Survey.

654

## 655 **References**

- 656 Antoine P, Lautridou JP, Sommé J, Auguste P, Auffret JP, Baize S, Clet-Pellerin M, Coutard JP, Dewolf Y, Dugué  
657 O, Joly F, Laignel B, Laurent M, Lavollé M, Lebreton P, Lécollé F, Lefebvre D, Limondin-Lozouet N, Munaut  
658 André V, Ozouf JC, Quesnel F, Rousseau DD. 1998. Les formations quaternaires de la France du Nord-Ouest:  
659 Limites et corrélations. *Quaternaire* **9**(3): 227–241.
- 660 Antoine P, Lautridou JP, Laurent M. 2000. Long-Term Fluvial archives in NW France: response of the Seine and  
661 Somme Rivers to Tectonic movements, Climatic variations and Sea level changes. *Geomorphology* **33**: 183–207.
- 662 Antoine P, Coutard JP, Gibbard P, Hallegouet B, Lautridou JP, Ozouf JC, 2003. The Pleistocene rivers of the English  
663 Channel region. *Journal of Quaternary Science* **18**(3-4): 227–243.
- 664 Antoine P, Lozouet NL, Chaussé C, Lautridou JP, Pastre JF, Auguste P, Bahain JJ, Falguères C, Galle B. 2007.  
665 Pleistocene fluvial terraces from northern France (Seine, Yonne, Somme): synthesis, and new results from  
666 interglacial deposits. *Quaternary Science Reviews* **26**: 2701–2723.
- 667 Antoine P, Coutard S, Guerin G, Deschodt L, Goval E, Loch JL, Paris C. 2016. Upper Pleistocene loess-palaeosol  
668 records from Northern France in the European context: Environmental background and dating of the Middle  
669 Palaeolithic. *Quaternary International* **411**: 4–24.
- 670 Audra P, Palmer AN. 2013. The vertical dimension of karst: controls of vertical cave pattern. In *Treatise On*  
671 *Geomorphology*, Shroder J.F. (ed.), Elsevier academic press: Amsterdam;186–206.
- 672 Aranburu A, Arriolabengoa M, Iriarte E, Giralt S, Yusta I, Martínez-Pillado V, Del Val M, Moreno J, Jiménez-Sánchez  
673 M. 2014. Karst landscape evolution in the littoral area of the Bay of Biscay (north Iberian Peninsula). *Quaternary*  
674 *International* **367**: 217–230.
- 675 Atkinson TC, Rowe PJ. 1992. Applications of dating to denudation chronology and landscape evolution. In *Uranium*  
676 *series Disequilibrium: Applications to Earth, Marine and Environmental Sciences*, Ivanovich M, Harmon RS  
677 (eds.), Oxford University Press: Oxford; 669–703.
- 678 Balescu S, Lamothe M, Lautridou JP. 1997. Luminescence evidence for two Middle Pleistocene interglacial events at  
679 Tourville, northwestern France. *Boreas* **26**(1): 61–72.
- 680 Ballesteros D, Jiménez-Sánchez M, Giralt S, García-Sanseguendo J, Meléndez-Asensio M. 2015. A multi-method  
681 approach for speleogenetic research on alpine karst caves. Torca La Texa shaft, Picos de Europa (Spain).  
682 *Geomorphology* **247**: 35–54.
- 683 Bella P, Bosák P, Braucher R, Pruner P., Hercman H., Minár J, Veselský M, Holec J, Léanni L. 2019. Multi-level  
684 Dómica–Baradla cave system (Slovakia, Hungary): Middle Pliocene–Pleistocene evolution and implications for  
685 the denudation chronology of the Western Carpathians. *Geomorphology* **327**: 62–79.
- 686 Bischoff JL, Julià R, Mora R. 1988. Uranium series dating of the Mousterian occupation at Abric Romaní, Spain.  
687 *Nature* **332** : 68–70.
- 688 Bridgland DR. 2000. River terrace systems in north-west Europe: an archive of environmental change, uplift and early  
689 human occupation. *Quaternary Science Reviews* **19**(13): 1293-1303.

- 690 Bridgland DR, Maddy D. 2002. Global correlation of long Quaternary fluvial sequences: a review of baseline  
691 knowledge and possible methods and criteria for establishing a database. *Netherlands Journal of*  
692 *Geosciences* **81**(3-4): 265-281.
- 693 Bridgland DR and Westaway R. 2008. Climatically controlled river terrace staircases: a worldwide Quaternary  
694 phenomenon. *Geomorphology* **98**: 285–315.
- 695 Calvet M, Gunnell Y, Braucher R, Hez G, Bourlès D, Guillou V, Delmas M. 2015. Cave levels as a proxy for  
696 measuring post-orogenic uplift: Evidence from cosmogenic dating of alluvium-filled caves in the French  
697 Pyrenees. *Geomorphology* **246**: 617–633.
- 698 Cande SC, Kent DV. 1995. Revised calibration of the geomagnetic polarity time scale for the late Cretaceous and  
699 Cenozoic. *Journal Geophysical Research* **100**: 6093–6095.
- 700 Chédeville S, Laignel B, Rodet J, Todisco D, Fournier M, Dupuis E, Girot G, Hanin G. 2015. The sedimentary filling  
701 in the chalk karst of the Northwestern Paris Basin (Normandy, France): Characterization, origin and hydro-  
702 sedimentary behaviour. *Zeitschrift für Geomorphologie* **59**: 79–101.
- 703 Cheng H, Edwards RL, Shen CC, Polyak VJ, Asmerom Y, Woodhead J, Hellstrom J, Wang Y, Kong X, Spötl C,  
704 Wang X. 2013. Improvements in  $^{230}\text{Th}$  dating,  $^{230}\text{Th}$  and  $^{234}\text{U}$  half-life values, and U–Th isotopic measurements  
705 by multi-collector inductively coupled plasma mass spectrometry. *Earth and Planetary Science Letters* **1**(371):  
706 82–91.
- 707 Cliquet D., Lautridou JP, Antoine P, Lamothe M, Leroyer M, Limondin-Lozouet N, Mercier N, 2009. La séquence  
708 loessique de Saint-Pierre-lès-Elbeuf (Normandie, France) : nouvelles données archéologiques,  
709 géochronologiques et paléontologiques. *Quaternaire* **20**(3) : 321–343.
- 710 Columbu A, De Waele J, Forti P, Montagna P, Picotti V, Pons-Branchu E, Hellstrom J, Bajo P, Drysdale RN. 2015.  
711 Gypsum caves as indicators of climate-driven river incision and aggradation in a rapidly uplifting region.  
712 *Geology* **43**(6): 539-542.
- 713 Constantin S, Lauritzen SE, Stiuca, E, Petculescu, A. 2001. Karst evolution in the Danube Gorge from U-series dating  
714 of a bear skull and calcite speleothems from Pestera de la Gura Ponicevei (Romania). *Theoretical and Applied*  
715 *Karstology* **13-14**, 39-50.
- 716 Coquerel G, Lefebvre D, Rodet J, Staigre JC. 1993. La Grotte du Funiculaire (Le Mesnil sous Jumièges, seine-  
717 Maritime). Spéléogénèse et étude d'un remplissage ferro-magnétique. *Karstologia* **22**: 35–42.
- 718 Dabkowski J, Limondin-Lozouet N, Antoine P, Andrews J, Marca-Bell A, Robert V. 2012. Climatic variations in MIS  
719 11 recorded by stable isotopes and trace elements in a French tufa (La Celle, Seine Valley). *Journal of Quaternary*  
720 *Sciences* **27**(8): 790-799.
- 721 Dugué O, Lautridou JP, Quesnel F, Clet M, Poupinet N, Bourdillon C. 2009. Évolution sédimentaire cénozoïque  
722 (Paléocène à Pleistocène inférieur) de la Normandie. *Quaternaire* **20**(3): 275–303.
- 723 Duperré A, Vandycke S, Mortimore RN, Genter A. 2012. How plate tectonics is recorded in chalk deposits along the  
724 eastern English Channel in Normandy (France) and Sussex (UK). *Tectonophysics* **581**: 163–181
- 725 Edwards RL, Chen JH, Ku TL, Wasserburg GJ. 1987. Precise timing of the last interglacial period from mass  
726 spectrometric determination of  $^{230}\text{Th}$  in corals. *Science* **236**: 1547–1553.
- 727 Ford DC, Schwarcz HP, Drake JJ, Gascoyne M, Harmon RS, Latham AG. 1981. Estimates of the age of the existing  
728 relief within the southern Rocky Mountains of Canada, Arctic. *Alpine Research* **13**: 1–10.
- 729 Filipponi M, Jeannin PY, Tacher L. 2009. Evidence of inception horizons in karst conduit networks. *Geomorphology*  
730 **106**: 86-99.

- 731 Farrant AR, Smart, PL. 2011. Role of sediments in speleogenesis; sedimentation and paragenesis. *Geomorphology*  
732 **134**: 79–93.
- 733 Farrant AR, Smart PL, Whitaker FF, Tarling DH. 1995. Long-term Quaternary uplift rates inferred from limestone  
734 caves in Sarawak, Malaysia. *Geology* **23**: 357–360.
- 735 Ford DF, Williams PW. 2007. *Karst Hydrogeology and Geomorphology*. Chichester, John Wiley & Sons.
- 736 Gabrovšek F, Häuselmann P, Audra P. 2014. ‘Looping caves’ versus ‘water table caves’: the role of base-level changes  
737 and recharge variations in cave development. *Geomorphology* **204**, 683–691.
- 738 Gibbard PL, Cohen KM. 2015. Quaternary evolution of the North Sea and the English Channel. *Proceedings of the*  
739 *Open University Geological Society* **1**: 63-74.
- 740 Granger DE, Fabel D, Palmer AN. 2001. Pliocene–Pleistocene incision of the Green River, Kentucky, determined  
741 from radioactive decay of cosmogenic <sup>26</sup>Al and <sup>10</sup>Be in Mammoth Cave sediments. *Geological Society of America*  
742 *Bulletin* **113**(7): 825–836.
- 743 Guillocheau F, Robin C, Allemand P, Bourquin S, Brault N, Dromart G, FriedenberG R, Garcia JP, Gaulier JM,  
744 Gaumet F, Grosdoy B, Hanot F, Le Strat P, Mettraux M, Nalpas T, Prijac C, Rigoltet C, Serrano O, Grandjean,  
745 G. 2000. Meso-cenozoic geodynamic evolution of the Paris Basin: 3d stratigraphic constraints. *Geodinamica Acta*  
746 **13**: 189–245.
- 747 Gupta, S., Collier, J.S., Garcia-Moreno, D., Oggioni, F., Trentesaux, A., Vanneste, K., De Batist, M., Camelbeeck, T.,  
748 Potter, G., Van Vliet-Lanoë, B. and Arthur, J.C., 2017. Two-stage opening of the Dover Strait and the origin of  
749 island Britain. *Nature Communications*, **8**: 15101.
- 750 Hajna NZ, Mihevc A, Pruner P, Bosák P. 2010. Palaeomagnetic research on karst sediments in Slovenia. *International*  
751 *Journal of Speleology* **39**(2): 47–60.
- 752 Harmand D, Adamson K, Rixhon G, Jaillet S, Losson B, Devos A, Hez G, Calvet M, Audra P. 2017. Relationships  
753 between fluvial evolution and karstification related to climatic, tectonic and eustatic forcing in temperate  
754 regions. *Quaternary Science Reviews* **166**: 38–56.
- 755 Hauchard E, Laignel B. 2008. Morphotectonic evolution of the north-western margin of the Paris Basin. *Zeitschrift*  
756 *für Geomorphologie* **52**(4): 463–488.
- 757 Häuselmann P, Lauritzen SE, Jeannin PY, Monbaron M. 2008. Glacier advances during the last 400 ka as evidenced  
758 in St. Beatus Caves (BE, Switzerland). *Quaternary International*, **189**(1): 173–189.
- 759 Heiss J, Condon DJ, McLean N, Noble SR. 2012. <sup>238</sup>U/<sup>235</sup>U systematics in terrestrial uranium-bearing minerals,  
760 *Science* **335**: 1610–1614.
- 761 Hellstrom J. 2006. U–Th dating of speleothems with high initial <sup>230</sup>Th using stratigraphical constraint. *Quaternary*  
762 *Geochronology* **1**: 289–295.
- 763 Jeannin PY, Eichenberger U, Sinreich M, Vouillamoz J, Malard A, Weber E. 2013. KARSYS: a pragmatic approach  
764 to karst hydrogeological system conceptualisation. Assessment of groundwater reserves and resources in  
765 Switzerland. *Environmental Earth Sciences* **69**: 999–1013.
- 766 Juignet P, Breton G. 1992. Mid-cretaceous sequence stratigraphy and sedimentary cyclicality in the western Paris Basin.  
767 *Palaeogeography Palaeoclimatology Palaeoecology* **91**: 197–218.
- 768 Kirschvink JL, Kopp RE, Raub TD, Baumgartner CT, Holt JW. 2008. Rapid, precise, and high-sensitivity acquisition  
769 of Palaeomagnetic and rock-magnetic data: development of a low-noise automatic sample changing system for  
770 superconducting rock magnetometers. *Geochemistry Geophysics Geosystem* **9**(5): 1–18.
- 771 Lagarde JL, Baize S, Amorese D, Delcaillau B, Font M, Volant P, 2000. Active tectonics, seismicity and  
772 geomorphology with special reference to Normandy (France). *Journal of Quaternary Science* **15**(7): 745–758.

- 773 Laignel B, Quesnel F, Meyer R. 1998. Variabilité du cortège argileux des formations résiduelles à silex de l'ouest du  
774 Bassin de Paris. *Compte Rendu de l'Académie des Sciences* **326**: 467–472.
- 775 Laignel B. 1997. Les altérites à silex de l'ouest du Bassin de Paris. Caractérisation lithologique, genèse et utilisation  
776 potentielle comme granulats, PhD thesis, Université de Rouen: 224.
- 777 Laignel B, Dupuis E, Rodet J, Lacroix L, Masséi N. 2004. An example of sedimentary filling in the chalk karst of  
778 the Western Paris Basin: characterization, origins and hydro-sedimentary behaviour. *Zeitschrift für*  
779 *Geomorphologie* **48**: 219–243.
- 780 Larue JP, Etienne R. 2000. Les Sables de Lozère dans le Bassin parisien : nouvelles interprétations. *Géologie de la*  
781 *France* **2**, 81-94.
- 782 Lasseur E, Guillocheau F, Robin C, Hanot F, Vaslet D, Coueffe R, Neraudeau D. 2009. A relative water-depth model  
783 for the Normandy Chalk (Cenomanian-Middle Coniacian, Paris Basin, France) based on facies patterns of metre-  
784 scale cycles. *Sedimentary Geology* **213**(1–2): 1–26.
- 785 Laureano FV, Karmann I, Darryl E, Granger DE, Auler AS, Almeida RP, Cruz FW, Stricks NM, Novello VF. 2016.  
786 Two million years of river and cave aggradation in NE Brazil: implications for speleogenesis and landscape  
787 evolution, *Geomorphology* **273**: 63–77.
- 788 Lauritzen SE, Lauritsen Å. 1995. Differential diagnosis of paragenetic and vadose canyons. *Cave and Karst Science*  
789 **21**: 55–59.
- 790 Lautridou JP. 1983. *Le Quaternaire de Normandie*. Éditions U.E.R. Sciences, Rouen, France.
- 791 Lautridou JP. 2003. La datation du Quaternaire normand: tableau des éléments de datation et de la chronostratigraphie.  
792 *Quaternaire* **14**(1): 65–71.
- 793 Lautridou JP, Lefebvre D, Lécolle F, Carpentier G, Descombes JC, Gaquerel C, Huault MF. 1984. Les Terrasses de  
794 la Seine dans le méandre d'Elbeuf, corrélations avec celles de la région de Mantes. *Bulletin de l'Association*  
795 *Française pour l'Étude du Quaternaire* **3** : 27–32.
- 796 Lautridou JP, Auffret JP, Lecolle F, Lefebvre D, Lericolais G, Roblin-Jouve A, Balescu S, Carpentier G, Cordy JM,  
797 Descombes JC, Occhietti S, Rousseau DD. 1999. Le fleuve Seine, Le fleuve Manche. *Bulletin de la Société*  
798 *Géologique de France* **170**: 545–558.
- 799 Lécolle F. 1989. *Le cours moyen de la Seine au pléistocène moyen et supérieur, géologie et préhistoire*. Thèse d'État,  
800 Université de Paris VI (1987). Groupe Seine, Laboratoire de Géologie Université de Rouen. 1–549.
- 801 Lefebvre D, Antoine P, Auffret JP, Lautridou JP, Lécolle F. 1994. Rythme de réponse des environnements fluviaux  
802 aux changements climatiques en France du Nord-Ouest. *Quaternaire* **5**(3–4): 165–172.
- 803 Lowe D. 2000. Role of Stratigraphic Elements. In: Klimchouk A, Ford DF, Palmer AN, Dreybrodt W (eds).  
804 *Speleogenesis: The Speleoinception Concept*. Speleogenesis. Evolution of Karst Aquifers. Huntsville,  
805 National Speleological Society; 65–76.
- 806 Luiszer FG. 1999. Speleogenesis of Cave of the Winds, Manitou Springs, Colorado. In *Breakthroughs in Karst*  
807 *Geomicrobiology and Redox Geochemistry*, Sasowsky ID, Palmer MV (eds). Journal Karst Waters Institut:  
808 Charles Town, Special Publication; 91–109.
- 809 Mortimore RN. 2018. Late Cretaceous to Miocene and Quaternary deformation history of the Chalk: Channels,  
810 slumps, faults, folds and glaciectonics. *Proceedings of the Geologists' Association* **130**: 27–65.
- 811 Nehme C, Jaillet S, Voisin C, Hellstrom J, Gérard-Adjizian J, Delannoy JJ. 2016. Control of cave levels in Kanaan,  
812 Kassarat and Jeita karst systems (Central Mount Lebanon, Lebanon). *Zeitschrift für Geomorphologie* **60**(2): 95–  
813 117.
- 814 Palmer AN. 1987. Cave levels and their interpretation. *National Speleological Society Bulletin* **49**: 50–66.

- 815 Palmer AN. 1991. Origin and morphology of limestone caves. *Geological Society America Bulletin* **103**: 1–21.
- 816 Pasini G. 2009. A terminological matter: paragenesis, antigravitative erosion or antigravitational erosion?  
817 *International Journal of Speleology* **38**: 129–138.
- 818 Pedoja K, Jara-Muñoz J, De Gelder G, Robertson J, Meschis M, Fernandez-Blanco D, Nexer M, Poprawski Y, Dugué  
819 O, Delcaillau B, Bessin P, Benabdelouahed M, Authemayou C, Husson L, Regard V, Menier D, Pinel B. 2018.  
820 Neogene-Quaternary slow coastal uplift of Western Europe through the perspective of sequences of strandlines  
821 from the Cotentin Peninsula (Normandy, France). *Geomorphology* **303**: 338–356.
- 822 Pennos C, Lauritzen SE, Pechlivanidou S, Sotiriadis Y. 2016. Geomorphic constrains on the evolution of the Aggitis  
823 River Basin Northern Greece (a preliminary report). *Bulletin of the Geological Society of Greece* **50**(1): 365–373.
- 824 Piccini L, Landelli N. 2011. Tectonic uplift, sea level changes and Plio-Pleistocene evolution of a coastal karst system:  
825 the Mount Saint Paul (Palawan, Philippines). *Earth Surface Processes and Landforms*, **36**(5): 594–609.
- 826 Plan L, Filipponi M, Behm M, Seebacher R, Jeutter P. 2009. Constraints on alpine speleogenesis from cave  
827 morphology - A case study from the eastern Totes Gebirge (Northern Calcareous Alps, Austria). *Geomorphology*  
828 **106**: 118–129.
- 829 Quesnel F, Catt J, Laignel B, Bourdillon C, Meyer R. 2003. The Neogene and Quaternary Clay-with-flints north and  
830 south of the English Channel: comparisons of distribution, age, genetic processes and geodynamics. *Journal of*  
831 *Quaternary Science*. **18**(3-4): 283–294.
- 832 Renault P. 1968. Contribution à l'étude des actions mécaniques et sédimentologiques dans la spéléogénèse. Les  
833 facteurs sédimentologiques. *Annales de Spéléologie* **23**: 529–593.
- 834 Robin C, Allemand P, Burov E, Doin MP, Guillocheau F, Dromart G, Garcia JP. 2003. Vertical movements of the  
835 Paris Basin (Triassic-Pleistocene): From 3D stratigraphic database to numerical models. IN: Nieuwland DA (ed).  
836 *New Insights into Structural Interpretation and Modelling*. Geological Society, London, Special Publications 212;  
837 225-250.
- 838 Rodet J. 1992. *La Craie et ses karsts*. Groupe Seine et Centre Normand d'Etude du Karst et des Cavités du Sous-Sol  
839 Elbeuf, France.
- 840 Rodet J. 2007. Karst de la craie et aquifère de Normandie. *European Journal of Water Quality* **38**: 11–22.
- 841 Rodet J, Lautridou J. 2003. Contrôle du karst quaternaire sur la genèse et l'évolution du trait de côte d'une région  
842 crayeuse de la Manche (Pays de Caux, Normandie, France). *Quaternaire* **14**:31-42.
- 843 Rodet J, Laignel B, Brocard G, Dupuis E, Massei N, Viard J. 2006. Contribution of a sedimentary study to the concept  
844 of karstic evolution of a chalk cave in the western Paris basin (Normandy, France). *Geologica Belgica* **9**: 287–  
845 296.
- 846 Rossi C, Villalaín JJ, Lozano RP, Hellstrom J. 2016. Paleo-watertable definition using cave ferromanganese  
847 stromatolites and associated cave-wall notches (Sierra de Arnero, Spain). *Geomorphology* **261**: 57–75.
- 848 Rousseau DD, Puissgur JJ, Lécolle F. 1992. West-European terrestrial molluscs assemblages of isotopic stage 11-  
849 Middle Pleistocene: climatic implications. *Palaeogeography Palaeoclimatology Palaeoecology* **92**: 15–19.
- 850 Sasowsky ID, White WB, Schmidt VA. 1995. Determination of stream-incision rate in the Appalachian plateaus by  
851 using cave-sediment magnetostratigraphy. *Geology* **23**: 415–418.
- 852 Sauro F, Zamperi D, Filipponi M. 2013. Development of a deep karst system within a transpressional structure of the  
853 Dolomites in north-east Italy. *Geomorphology* **184**: 51-63.
- 854 Singer BA. 2014. A Quaternary geomagnetic instability time scale. *Quaternary Geochronology* **21**: 29-52.
- 855 Skoglund RØ, Lauritzen SE. 2010. Morphology and speleogenesis of Okshola (Fauske, northern Norway): example  
856 of a multi-stage network cave in a glacial landscape. *Norwegian Journal of Geology* **90**: 123–139.

- 857 Stock GM, Granger DE, Sasowsky ID, Anderson RS, Finkel RC. 2005. Comparison of U–Th, paleomagnetism, and  
858 cosmogenic burial methods for dating caves: implications for landscape evolution studies. *Earth and Planetary*  
859 *Science Letters* **236**(1-2): 388–403.
- 860 Tofelde S, Savi S, Wickert AD, Bufe A and Schildgen TF. 2019. Alluvial channel response to environmental  
861 perturbations: fill-terrace formation and sediment-signal disruption. *Earth Surface Dynamics*, **7**(2): 609–631.
- 862 Tourenq J, Pomerol C, 1995. Mise en évidence par la présence d’augite du Massif Central, de l’existence d’une pre  
863 Loire - pre Seine coulant vers la Manche au Pleistocene. *Compte Rendu de l’Académie de Sciences de Paris*  
864 **320**(IIa): 1163–1169.
- 865 Valdes, D., Dupont, JP., Laignel, B, Slimani, S, Delbart, C. 2014. Infiltration processes in karstic chalk investigated  
866 through a spatial analysis of the geochemical properties of the groundwater: The effect of the superficial layer of  
867 clay-with-flints. *Journal of Hydrology*, **519**: 23–33.
- 868 Van Vliet-Lanoë B, Vandenberghe N, Laurent M, Laignel B, Lauriat-Rage A, Louwye S, Mansy JL, Mercier D,  
869 Hallégouët B, Laga P, Laquement F. 2002. Palaeogeographic evolution of northwestern Europe during the Upper  
870 Cenozoic. *Geodiversitas* **24**(3): 511-541.
- 871 Westaway R. 2004. Pliocene and Quaternary surface uplift evidenced by sediments of the Loire Allier river system  
872 (France). *Quaternaire* **15**(1): 103–115.